ELSEVIER

Advanced Drug Delivery Reviews 50 (2001) S41–S67

Advanced DRUG DELIVERY Reviews

www.elsevier.com/locate/drugdeliv

Predicting the impact of physiological and biochemical processes on oral drug bioavailability

Balaji Agoram[a], Walter S. Woltosz[a], Michael B. Bolger[a,b,*]

[a]*Simulations Plus, Inc. 1220 W. Avenue J, Lancaster, CA 93534-2902, USA*
[b]*Department of Pharmaceutical Sciences, USC School of Pharmacy, 1985 Zonal Ave. PSC 700, Los Angeles, CA 90089-9121, USA*

Abstract

Recent advances in computational methods applied to the fields of drug delivery and biopharmaceutics will be reviewed with a focus on prediction of the impact of physiological and biochemical factors on simulation of gastrointestinal absorption and bioavailability. Our application of a gastrointestinal simulation for the prediction of oral drug absorption and bioavailability will be described. First, we collected literature data or we estimated biopharmaceutical properties by application of statistical methods to a set of 2D and 3D molecular descriptors. Second, we integrated the differential equations for an advanced compartmental absorption and transit (ACAT) model in order to determine the rate, extent, and approximate gastrointestinal location of drug liberation (for controlled release), dissolution, passive and carrier-mediated absorption, and saturable metabolism and efflux. We predict fraction absorbed, bioavailability, and C_p vs. time profiles for common drugs and compare those estimates to literature data. We illustrate the simulated impact of physiological and biochemical processes on oral drug bioavailability. © 2001 Elsevier Science B.V. All rights reserved.

Keywords: Carrier-mediated transport and efflux; Saturable P450 metabolism; In silico simulation; Drug absorption

Contents

*Corresponding author. Tel.: +1-323-442-1442; fax: +1-323-442-3656.
E-mail address: bolger@usc.edu (M.B. Bolger).

0169-409X/01/$ – see front matter © 2001 Elsevier Science B.V. All rights reserved.
PII: S0169-409X(01)00179-X

1. Introduction

Application of computational technology during drug discovery and development has the potential to decrease the length of time prior to NDA submission, and reduce the number of experimental procedures required for compound selection and development. Oral bioavailability can be broken down into components that reflect delivery to the intestine (gastric emptying, intestinal transit, local pH, and nutritional status), absorption from the lumen (dissolution, permeability, particle size, intestinal efflux and carrier-mediated transport), first-pass metabolism in the gut, and subsequent first-pass hepatic extraction [1]. Both experimental in vitro and estimated in silico biopharmaceutical properties can be used to predict drug absorption, distribution, metabolism, excretion, and toxicity (ADMET). This review will focus on in silico approaches that have the potential to save valuable resources in drug discovery and development. We review methods that have been developed to build models of individual biopharmaceutical properties, followed by a review of theoretical methods employed to simulate gastrointestinal absorption, hepatic and intestinal metabolism, and pharmacokinetics. Finally, we present our results in predicting bioavailability by estimating biopharmaceutical properties and simulating gastrointestinal absorption and metabolism by extending the advanced compartmental absorption and transit (ACAT) model to account for nonlinear saturable processes.

2. Computer models of biopharmaceutical properties

In order to lessen the expense and decrease the time associated with experimental determination of in vitro biopharmaceutical properties, existing data has been used to build computational models of octanol–water partition coefficient ($\log P$), effective human jejunal permeability (P_{eff}), cell culture permeability (Caco-2 or MDCK), aqueous solubility, and molecular diffusivity. These models have been developed by application of statistical methods such as linear and partial least squares (PLS) and artificial neural networks (ANN) to sets of molecular descriptors or molecular fragments derived from 2D and 3D molecular structures. When coupled to a physiologically based simulation of dissolution, gastrointestinal transit, absorption, and metabolism, the in vitro data or the in silico properties allow prediction of oral fraction absorbed and bioavailability. We have developed an application that will estimate biopharmaceutical properties such as human effective permeability, pure aqueous solubility, octanol–water partition coefficient, and molecular diffusivity. This application will be described in detail elsewhere (manuscript in preparation).

3. Simulation of oral drug absorption

Absorption of drugs from the gastrointestinal (GI) tract is very complex and can be influenced by many factors that fall into three classes [2]. The first class represents physicochemical factors including pK_a, solubility, stability, diffusivity, lipophilicity, and salt forms. The second class comprises physiological factors including GI pH, gastric emptying, small and large bowel transit times, active transport and efflux, and gut wall metabolism. The third class comprises formulation factors such as surface area, drug particle size and crystal form, and dosage forms such as solution, tablet, capsule, suspension, emulsion, gel, and modified release.

One of the original concepts governing oral absorption of organic molecules is called the 'pH-partition' hypothesis. Under this hypothesis, only the unionized form of ionizable molecules is thought to partition into the membranes of epithelial cells lining the GI tract [3,4]. Testing of this hypothesis has resulted in recognition of the important contribution of GI pH to permeability and to the dissolution rate of solid dosage forms, but it has not been found to be universally applicable. Ho and colleagues developed one of the most sophisticated early theoretical approaches to simulating drug absorption based on the diffusional transport of drugs across a compartmental membrane [5–7]. Their physical model consisted of a well-stirred bulk aqueous phase, an aqueous diffusion layer, and a heterogeneous lipid barrier composed of several compartments ending in a perfect sink. Their model represented the first example of the rigorous application of a physical model to the quantitative and mechanistic interpretation of in vivo absorption [8]. The simultaneous chemical equilibria and mass transfer of basic and acidic drugs were modeled and compared favorably to in situ measurements of intestinal, gastric, and rectal absorption in animals. The pH-partition theory was shown to be a limiting case of the more general model they developed. Because of its complexity, the diffusional mass transit model has not been widely utilized. In the 1980s, a simple and intuitive alternative approach based on a series of mixing tank compartments was developed [9]. Pharmacokinetic models incorporating discontinuous GI absorption from at least two absorption sites separated by N non-absorbing sites have been used to explain the occurrence of double peaks in plasma concentration vs. time (C_p–time) profiles for ranitidine and cimetidine [10]. A similar discontinuous oral absorption model based on two absorption compartments and two transit compartments was developed to explain the bioavailability of nucleoside analogs [11]. Finally, using a poorly described gastrointestinal simulation model, Norris et al. were able to estimate C_p–time profiles for ganciclovir [12].

Correct representation of the gastrointestinal tract as a series of compartments requires an analysis of small intestine (SI) transit time frequency distribution to determine the correct number of compartments. Analysis of more than 400 human SI transit times revealed a log normal distribution with mean SI transit time of 3.3 h [13]. In the case of no absorption or degradation, the cumulative distribution of transit time data set can be viewed as the percent of a dose entering the colon as a function of time (Fig. 1). By integrating the transit of material through the SI as represented by various numbers of compartments and plotting the cumulative amount that reaches the colon, Yu determined that seven

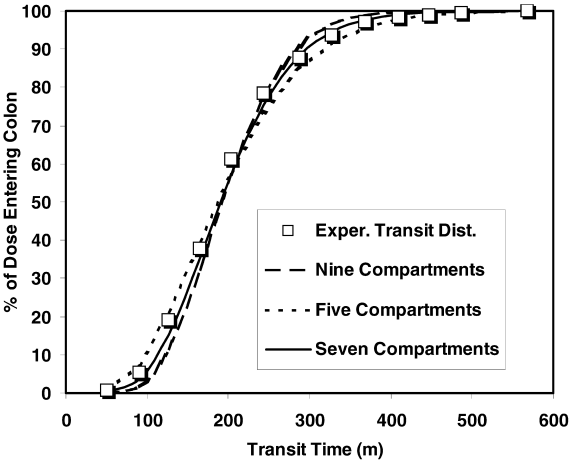

Fig. 1. Graphical representation of the small intestinal transit time distribution for 400 experimentally determined transit times [13]. Represents a frequency distribution plot of the mean small intestinal transit time in approximately 400 subjects. The cumulative transit time distribution was simulated using 5, 7, and 9 equal transit time compartments. The seven compartment model was found to give the best fit to observed data on cumulative appearance in the colon.

equal transit time small intestine compartments gave the best fit to the observed cumulative frequency distribution. The seven-compartment transit model may be visualized as having the first half of the first compartment representing the duodenum, the second half of the first compartment, along with the second and third representing the jejunum, and the rest representing the ileum. The corresponding transit times in the duodenum, jejunum, and ileum are 14, 71, and 114 min.

Based on this transit time distribution for seven SI compartments, Yu and Amidon developed a compartmental absorption and transit (CAT) model to simulate the rate and extent of drug absorption [2]. The CAT model is described by a set of differential equations that considers simultaneous movement of a drug in solution through the GI tract and absorption of the dissolved material from each compartment into the portal vein. The rate constant for absorption from each compartment is based on measured values of H–P_{eff}. Both analytical and numerical methods have been used to solve the model equations. It was found that the fraction of dose absorbed for drug in solution can be estimated by using a simple equation. A good correlation was found between the fraction of dose absorbed and the effective permeability for ten drugs covering a wide range of absorption characteristics when the effects of drug dissolution and dosage form could be neglected. The model was also able to explain the oral plasma concentration profiles of atenolol [14]. The CAT model has proven to be more versatile than earlier aggregate models such as the single-tank mixing model and the macroscopic or microscopic mass balance models [15,16].

Subsequently, a similar gastrointestinal transit and segmental absorption model based on five SI segments plus the caecum and the large intestine coupled to a two compartment pharmacokinetic (PK) model, was used to simulate the plasma concentration vs. time (C_{p}-time) profiles for ampicillin, theophylline, propranolol, and cephalexin [17]. The propranolol C_{p}–time profile was overestimated because first pass metabolism (approximately 58% for propranolol) was not considered in the PK model. Another method based on the CAT model that utilizes in vitro measurements of biopharmaceutical properties has been used to simulate the absorption of ganciclovir. The authors concluded from their simulation results that the low bioavailability of ganciclovir is limited by compound solubility rather than permeability due to partitioning as previously speculated [12].

Macheras has developed the heterogeneous tube model of the small intestine based on a stochastic simulation of drug molecules moving through a cylinder of fixed radius with random geometric placement of dendritic-type virtual ‘villi’. Drug molecules are assigned a probability of forward movement using a Monte Carlo blind ant random walk simulation. Contact between the drug molecule and virtual villi impede the movement causing dispersion of the mass of drug as it passes through the cylinder. This model has been calibrated to accurately account for the observed human SI transit time distribution [18,19].

Recently, a theory of molecular absorption from the small intestine based on macrotransport analysis has resulted in a model that includes complex interrelationships between lumen and membrane diffusion, convection, degradation and absorption mechanisms [20]. Finally, Ito et al. have developed a pharmacokinetic model for drug absorption that includes metabolism by CYP3A4 inside the epithelial cells, P-gp-mediated efflux into the lumen, intracellular diffusion from the luminal side to the basal side, and subsequent permeation through the basal membrane [21]. As expected, they demonstrated that the fraction absorbed was synergistically elevated by simultaneous inhibition of both CYP3A4 and P-gp.

3.1. Advanced CAT (ACAT) model

The published version of the original CAT model does not account for dissolution rate, the pH dependence of solubility, controlled release, absorption in the stomach or colon, metabolism in gut or liver, degradation in the lumen, or such factors as changes in absorption surface area, transporter densities, efflux protein densities, and other regional factors within the intestinal tract. For drugs with low permeability or solubility, absorption may not be complete in the small intestine and the CAT model can be made more accurate by treating the colon as an additional absorbing compartment. For drugs with

high permeability and high solubility, colonic absorption is a negligible fraction of the total absorption for immediate release formulations; however, for many immediate release drugs with moderate to low permeability and for most controlled release formulations, colonic absorption can be significant. We have now extended the CAT model to include these effects. GastroPlus™ is a simulation software product based on a new model, which is called the advanced CAT (ACAT) model (Fig. 2). As with the original CAT model, a basic assumption of the ACAT model is that drug passing through the small intestine will have equal transit time in each of the seven compartments. Since the volume of fluid entering the small intestine (8–9 l/day) in the duodenum and jejunum is more than the amount that exits the SI (0.5–1 l/day), then to satisfy the equal transit time constraint, volumes and transit rates of the upper SI compartments are considered to be larger than the lower compartments. The luminal barrier, which was treated using the 'thin wall' assumption in the original CAT model, has been modified by the addition of compartments corresponding to the enterocytes and surrounding tissues. In addition, the ACAT model uses the concentration gradient across the apical and basolateral membranes to calculate the rate of drug transfer into and out of an enterocyte compartment for each GI tract lumen compartment, whereas the CAT model assumed drug transfer to be unidirectional – lumen to central compartment. Thus, drug can move in either direction depending on the concentration gradient. It can be passively secreted back into the lumen – even from an intravenous dose – and more closely simulates in vivo results [22–24].

3.2. Numerical integration of ACAT

The form of the ACAT model implemented in GastroPlus™ describes the release, dissolution, luminal degradation (if any), metabolism, and absorption/exsorption of a drug as it transits through successive compartments. The kinetics associated with these processes are modeled by a system of

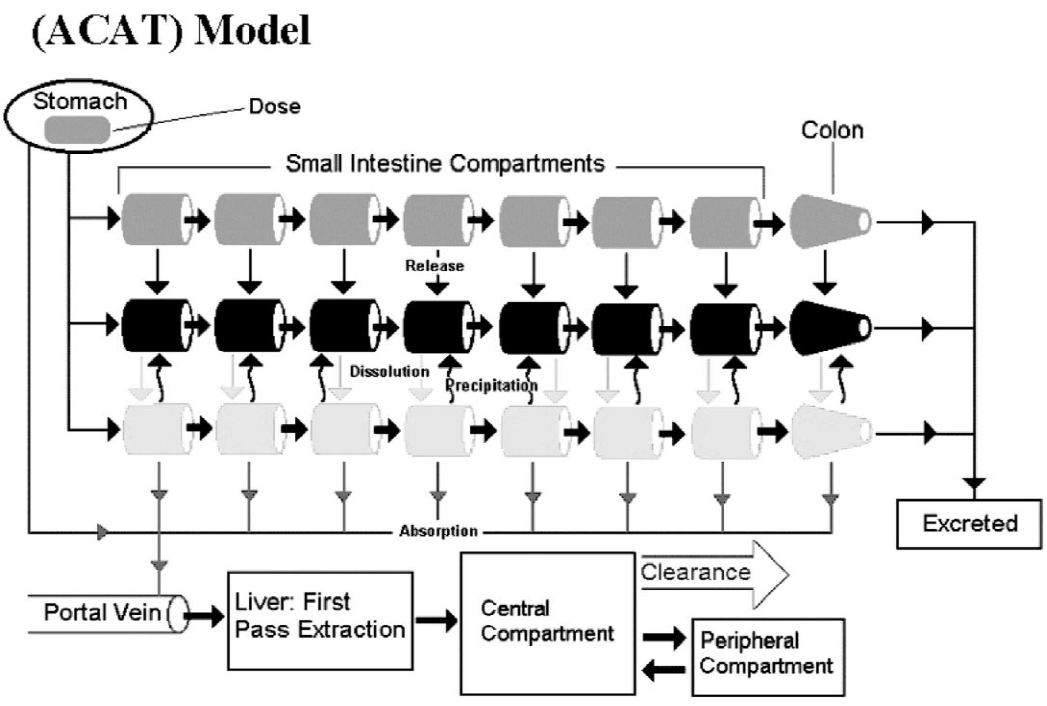

Fig. 2. ACAT model schematic. The original CAT model with seven compartments was modified to include compartment-dependent physiological parameters and the colon. One to three compartment pharmacokinetic models were also included to estimate C_p–time profiles.

coupled linear and non-linear rate equations. The equations include the consideration of six states (unreleased, undissolved, dissolved, degraded, metabolized, and absorbed), 18 compartments (nine GI (stomach, seven SI, and colon) and nine enterocyte), three states of excreted material (unreleased, undissolved, and dissolved), and the amount of drug in up to three pharmacokinetic compartments (when pharmacokinetic parameters are available). The total amount of absorbed material is summed over the integrated amounts being absorbed/exsorbed from each absorption/transit compartment.

In general, the rate of change of dissolved drug concentration in a luminal GI compartment depends on six different processes: (1) transit of drug into a compartment; (2) transit of drug out of a compartment; (3) release of drug from the formulation in the compartment; (4) dissolution/precipitation of drug particles; (5) luminal degradation of the drug; and (6) absorption/exsorption of the drug. The time scale associated with luminal transit is set by a transfer rate constant, k_t that is determined from the mean transit time within each compartment. The time scale of the dissolution process is set by a rate constant, k_d, that is computed from a drug's solubility (as a function of pH), its effective particle size, its particle density, its lumen concentration, its diffusion coefficient, and the diffusion layer thickness Eq. (1). The time scale associated with the absorption process is set by a rate constant, k_a, that depends on the effective permeability of the drug (P_{eff}, units of cm s^{-1}) multiplied by an absorption scale factor (ASF with units of cm^{-1}) for each compartment Eq. (2). The ASF corrects for changes in permeability due to changing physiology along the GI tract; e.g. absorption surface area, pH, and transport/efflux protein densities. The rates of absorption and exsorption depend on the concentration gradients across the apical and basolateral enterocyte membranes (Eqs. (3) and (4)). The time scale for luminal degradation is set by a rate constant, k_{Degrad} that is determined by interpolation from an input table of degradation rate (or half-life) vs. pH, and the pH in the compartment.

The system of differential equations is integrated using a 4th/5th order Runge–Kutta numerical integration package with adaptive step size [25]. The fraction of dose absorbed is calculated as the sum of all drug amounts disappearing from the GI tract as a function of time, divided by the dose, or by the sum of all doses if multiple dosing is used. Bioavailability is defined as the fraction of dose reaching the systemic circulation.

$$k_{(i)d} = 3\gamma \frac{C_S - C_{(i)L}}{\rho r T} \quad (1)$$

$$k_{(i)a} = \alpha(i) P_{eff} \quad (2)$$

$$\text{Absorption/Exsorption}_{(i)} = k_{(i)a} V_{(i)} \left(C_{(i)L} - C_{(i)E}\right) \quad (3)$$

$$\text{Basolateral transfer}_{(i)} = k'_{(i)a} V_{(i)} \left(C_{(i)E} - C_P\right) \quad (4)$$

where: $k_{(i)d}$, dissolution rate constant for the ith compartment; $k_{(i)a}$, absorption rate coefficient for the ith compartment; $k'_{(i)a}$, absorption rate coefficient specific for the basolateral membrane of the ith compartment; C_S, aqueous solubility; $C_{(i)L}$, lumen concentration for the ith compartment; $C_{(i)E}$, intracellular enterocyte concentration for the ith compartment; C_P, plasma central compartment concentration; V, volume of luminal compartment; γ, molecular diffusion coefficient; ρ, drug particle density; r, effective drug particle radius; T, diffusion layer thickness; α, compartmental absorption scale factor; and P_{eff}, human effective permeability.

3.3. Automatic scaling of k_a as a function of P_{eff}, pH, and log D

For passive diffusion, the size and shape of a drug molecule, its acid and base dissociation constants, and the pH of the gastrointestinal tract all influence the absorption rate coefficient for specific regions of the GI tract. Pade and coworkers measured the Caco-2 cellular permeability for a diverse set of acidic and basic drug molecules at two pH values [26]. They concluded that the permeability coefficients of the acidic drugs was greater at pH 5.4, whereas that of the basic drugs was greater at pH 7.2 and the transcellular pathway was the favored pathway for most drugs, probably due to its larger accessible surface area. The paracellular permeability of the drugs was size- and charge-dependent. The permeability of the drugs through the tight junctions decreased with increasing molecular size. Further,

the pathway also appeared to be cation-selective, with the positively charged cations of weak bases permeating the aqueous pores of the paracellular pathway at a faster rate than the negatively charged anions of weak acids. Thus, the extent to which the paracellular and transcellular routes are utilized in drug transport is influenced by the fraction of ionized and unionized species (which in turn depends upon the pK_a of the drug and the pH of the solution), the intrinsic partition coefficient of the drug, the size of the molecule and its charge.

Fig. 3 is a representation of regional permeability coefficients of 19 drugs with different physicochemical properties determined by Ungell et al. using excised segments from three regions of rat intestine: jejunum, ileum, and colon [27].

They observed a significant decrease in permeability to hydrophilic drugs and a significant increase in permeability for hydrophobic drugs aborally to the small intestine ($P = 0.0001$). Fig. 3 illustrates that for hydrophilic drugs (low permeability and low $\log D$) the ratio of colonic:jejunal permeability was less than one. While for hydrophobic drugs (higher permeability and higher $\log D$) the ratio of colonic:jejunal permeability is observed to be greater than one. At certain pH values the permeability of small hydrophilic drugs may have a large paracellular component [28] and it is well known that the transepithelial electrical resistance (TEER) of colon is much higher than small intestine. TEER increases as the width of tight junctions decrease and the tight junction width has been determined to be 0.75–0.8 nm in jejunum, 0.3–0.35 nm in ileum, and 0.2–0.25 nm in colon. The narrower tight junctions in colon suggest that paracellular transport will be much less significant in the colon, which helps to explain the lower ratio of colon:jejunal permeability for hydrophilic drugs. We have used the ACAT model with experimental biopharmaceutical properties for a series of hydrophilic and hydrophobic drug molecules to calibrate a 'log D model' that adjusts the absorption rate coefficient in each compartment according to pH and $\log D$ to explain the observed rate and extent of absorption.

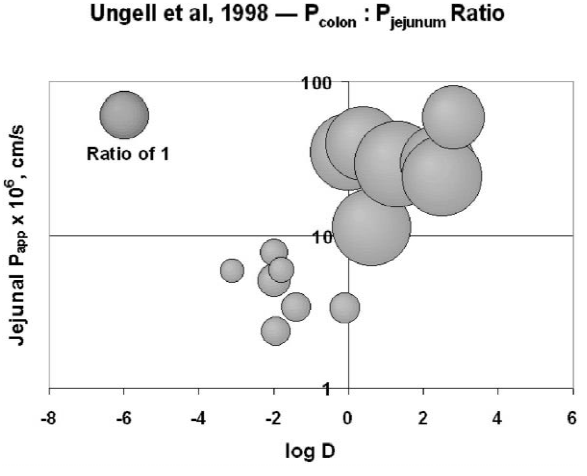

Fig. 3. Regional permeability from isolated rat gastrointestinal epithelial tissue as a function of log D for a small database of drug molecules. This figure is a replot of data from Ungell et al. who reported that the colonic permeability for lipophilic drugs was found to be higher than the jejunal permeability and the reverse was true for hydrophilic drugs [27].

4. Metabolism and first pass extraction

The various steps involved in oral drug absorption – dissolution, transit, drug transport and clearance have been traditionally assumed to be first-order non-saturable processes [17]. In reality, some processes are enzyme- or transporter-catalyzed, and they exhibit saturable, nonlinear kinetics. These processes include hepatic and intestinal metabolism, active efflux, and carrier-mediated transport. Apart from strongly influencing drug bioavailability, these nonlinear pharmacokinetic processes, especially metabolism, present many clinical complications. First pass elimination (FPE) refers to loss of a drug between the site of administration and the site of measurement of systemic concentration [29]. The loss can be due to biotransformation in one or more of the following sites: intestine, liver, and lungs. One major therapeutic implication of extensive first-pass elimination is that much larger oral doses than intravenous doses are required to achieve equivalent plasma concentrations. For some drugs, extensive first-pass metabolism precludes their therapeutic use by an oral route (e.g. lidocaine, naloxone) [29]. These drugs may also cause different metabolite concentration profiles based on the route of administration [30]. Drugs that undergo extensive FPE exhibit pro-

nounced inter-individual variability caused by varying enzyme activity due to induction, inhibition, genetic polymorphism, or disease state [31]. Because these drugs undergo nonlinear elimination, their bioavailability depends on the amount of the administered dose (e.g. propranolol), and the frequency and amount of subsequent doses (e.g. propranolol, acetaminophen). This disproportionate dose vs. plasma concentration relationship, coupled with high inter-individual variability, can cause potentially serious clinical effects.

4.1. Liver metabolism

Although FPE can occur anywhere from the gut to the liver, the liver is the most important organ for drug metabolism [29,32]. Because of its contribution in reducing the bioavailability of a drug, knowledge of hepatic first pass clearance is essential in assessing the therapeutic efficacy of a dosing regimen. Fig. 4 schematically represents the physiology of drug absorption and metabolism. Orally administered drugs enter the portal vein from the gastrointestinal tract and are transported to the liver. Intravenously administered drugs circulate through the system and enter the liver through both the portal vein and the hepatic artery. Extraction takes place in the hepatocytes and is usually due to enzyme-mediated reactions.

The cytochrome P-450 family of enzymes, discovered in 1964, form the most important family of enzymes that carry out oxidation of drugs and xenobiotics in the liver [33]. Many isoforms of P-450 enzymes (labeled 3A4, 2D6, 2C9, 2C19, 1A2, etc.) have been identified [34]. The rate of drug elimination in the liver depends on hepatic flow rate, intrinsic capacity of the enzymes to metabolize the drug, and drug binding to plasma proteins. Factors such as age, gender, disease states, enzyme induction and inhibition, genetic polymorphism and food effects have been implicated in causing variability in pharmacokinetics of drugs that undergo extensive first-pass metabolism [31].

Both physical and mathematical models have been developed to explain hepatic extraction. Among physical models, in vitro and animal models are the most commonly used. Kinetic parameters such as V_{max} and K_m can be determined in vitro using hepatocytes, microsomes, or liver slices extracted from the liver of humans and other laboratory animals. Intrinsic clearance ($CL_{int}=V_{max}/K_m$ under linear conditions) from these models can be con-

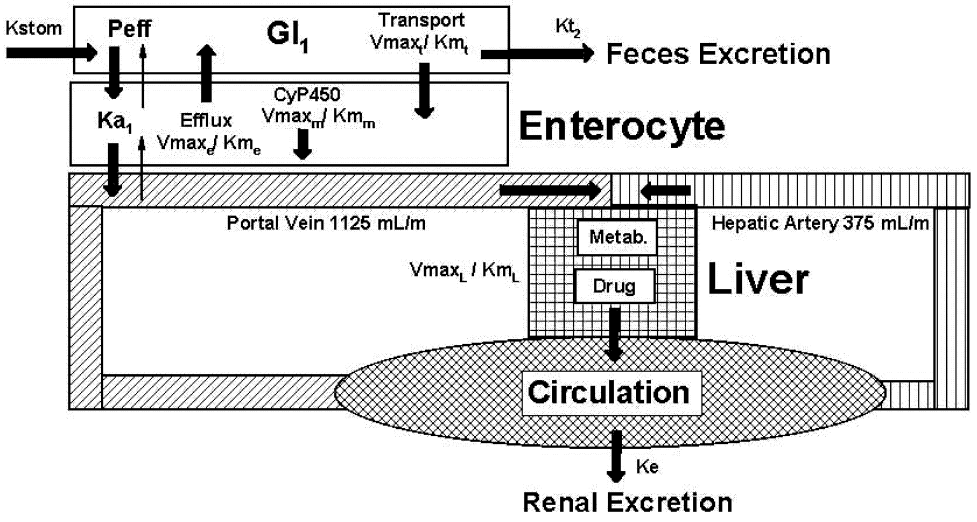

Fig. 4. Drug transfer from the lumen to the central compartment is schematically represented for one GI and enterocyte compartment. Drug transfer from the lumen to the enterocyte and from the enterocyte to systemic circulation is driven by their respective concentration gradients. P-gp efflux, and gut metabolism occur in the enterocytes. Circulating systemic drug and drug that has just been absorbed, both are subject to liver metabolism.

verted to an in vivo intrinsic clearance using various scaling methods based on the amount of enzyme present in vivo [35]. Often it is desirable to estimate clearance in humans from measurements in other species. This can be achieved using a method in which measurement of intrinsic hepatic clearance in one species is related to another species by empirical and physiological scaling [35,36]. Houston and Carlile have provided a comparison between in vitro methods using microsomes, hepatocytes, and liver slices to predict intrinsic clearance [37].

Once the in vivo intrinsic clearance is obtained by scaling in vitro clearance, a suitable mathematical model is chosen to describe the hepatic extraction of the drug. These mathematical models assume a concentration distribution of the drug in the liver based on the systemic concentration to explain distribution of drug through the liver sinusoids. Existing models of hepatic elimination may be classified according to their treatment of mixing within the vasculature and whether or not the model explicitly accounts for mass transfer between the heterogeneous phases of the liver. Saville et al. have defined four major classes of hepatic elimination models [38]:

1. Nonparametric homogeneous models, which assume that either complete mixing or no mixing occurs within the vasculature of the organ.
2. Homogeneous mixing models, which allow for a range of mixing phenomena.
3. Heterogeneous micromixing models, which allow for mass transport between the cells and vasculature and describe mixing within the vasculature on a microscopic level.
4. Heterogeneous compartmental models, which also describe interphase mass transfer but assume complete mixing on a microscopic level, and therefore use a time- and spatially-averaged approach to drug mixing [38].

Examples of the first case are the venous equilibrium model which assumes rapid and complete mixing in the liver sinusoids and the parallel tube model which assumes no mixing and plug-flow in the sinusoids. The dispersion model, an example of the second case, is intermediate to both venous equilibrium and plug flow models.

A number of drugs have been characterized in vivo using the above procedure [39]. Hoener obtained V_{max} and K_m values from in vitro metabolism experiments on human liver microsomes and calculated the hepatic clearance of a drug by a specific metabolic pathway. These parameters were scaled to physiological conditions using the mass of enzyme present in the cell and the in vivo clearances were calculated. The predictions agreed well with observed values for five compounds. Lave obtained a non-linear correlation between in vitro clearances calculated from hepatocytes and in vivo hepatic extraction ratio for 19 compounds [40]. Iwatsubo et al. predicted human pharmacokinetic profiles using physiologically based pharmacokinetic models after scale-up of physiological parameters from rat to human and found good agreement for an antidementia agent [41]. The same group also described a way to calculate in vivo intrinsic hepatic clearance from in vitro clearance data and found good correlation for 15 drugs under linear conditions [32]. They also developed a model for non-linear hepatic clearance assuming mono-exponential gastric emptying rate as the rate-limiting step in absorption and a dispersion model to describe drug concentration profile in the liver [42]. Their predictions for YM796 agreed well with literature values. Bogaards et al. predicted interindividual variation in plasma levels in vivo by scaling the in vitro enzyme kinetic parameters V_{max} and K_m and incorporating them into a physiologically-based pharmacokinetic model [43]. Schneider used artificial neural networks (ANN) to predict in vivo hepatic clearance in humans from hepatocyte data and found that human hepatocyte data was the best predictor, followed by rat hepatocyte data, while in vitro metabolism using dog hepatocytes was not predictive [44].

Although these methods predict drug elimination qualitatively, they have a few limitations regarding quantitative predictions. Most of them were developed for specific drugs and are applicable only under specific conditions, e.g. linearity, rapid absorption, specific dosage form, etc. Also, it is not easy to generalize these models across different physiological conditions (fed or fasted states), different dosage forms (immediate or extended release), or different pharmacokinetic behaviors (one/two/three compartment). Therefore, a generalized mathematical model

based on in vitro enzyme kinetic constants, and applicable under multiple physiological and dosage conditions would be a valuable tool in predicting behavior of drugs exhibiting nonlinear dose–response relationships.

4.2. Gut metabolism

The enterocytes present in the gut wall are well recognized as an additional site of first pass elimination of drugs and xenobiotics [31]. Individual variability in midazolam hydroxylation was shown to be highly correlated to the expression of CYP3A4 in the gut wall [45]. Activity of the gut wall enzymes, in general, is higher in the proximal parts and decreases distally [46]. Although the P-450 family of enzymes in the gut is present in much smaller quantities (~20 times less [33]), in some cases their contribution to metabolism of drugs is similar to that of the liver [22,46,47]. This fact is true particularly for drugs that are highly bound to plasma proteins and have limited access to the liver hepatocyte enzymes. Also, drugs with lower solubility or lower permeability that are substrates for CYP-3A metabolism are exposed to the gut enzymes for a longer period of time because their absorption time is slow relative to their transit time in the intestine. Since the enterocytes are more exposed to external factors such as food and substance intake, induction and inhibition of these enzymes by external agents cause significant intra- and inter-individual variations in their activity [46]. Intestinal metabolism is also known to be dependent on the route of administration, being higher during oral administration than during iv administration [48,49]. The liver and gut are usually assumed to be the major sites of first-pass metabolism of a drug administered orally, but other potential sites are blood, vascular endothelium, lungs, skin, and the arm from which venous samples are taken [29]. Drug metabolizing enzymes in the lungs have been reviewed by Baron and Voigt [50].

A few theoretical models exist that correlate physiological processes involving gut metabolism with overall drug absorption and bioavailability [21,49,51–53]. While these models describe route-dependent intestinal metabolism, they do not account for inter- and intra-individual variablity in enzyme distribution in the intestine. These models were also developed for specific drugs and their applicability to different drugs and different dosage forms remains a question.

4.3. Active efflux

The membrane-bound active efflux protein, P-glycoprotein (P-gp) is a product of the multidrug resistance gene mdr1 and has been shown to transport a large number of chemically diverse molecules. In the intestine, P-gp is expressed in the apical membrane of the enterocytes and acts as an absorption barrier by secreting drugs from the cell back into the lumen. Apart from the intestine, various forms of P-gp are present in almost all barrier tissues including, lungs, liver, kidneys, and blood brain barrier. Since the substrate specificity of P-gp and CYP3A4 overlap to some extent and since recently it has been discovered that these two proteins have a common regulatory mechanism, it has been suggested that they act synergistically in preventing drugs from crossing the intestinal barrier [54–56]. Drugs that enter the enterocyte are subject to metabolism by CYP3A4 and those that escape metabolism can be effluxed back into the lumen by P-gp where they could be absorbed again and be exposed to the enzymes. Apart from acting as an absorption barrier, the P-gp efflux system forms a significant clearance system for systemically administered drugs, e.g. digoxin and talinolol.

5. Bioavailability

Bioavailability is defined as the fraction of administered drug that reaches systemic circulation. Any loss could be due to any of the processes listed above – incomplete absorption, gut metabolism, liver metabolism, etc. If F_i is defined as the fraction of drug that escapes extraction at an organ (or process) i, then the overall bioavailability F is defined as

$$F = \prod_{i=1}^{n} F_i \tag{5}$$

In practice, bioavailability is defined as the ratio of the AUC's corrected for dose, after extra- and intravascular administration. The difference between

the AUC's is assumed to be a measure of first-pass elimination. So

$$F = \frac{\mathrm{AUC}_{\mathrm{oral}}}{\mathrm{AUC}_{\mathrm{iv}}} \frac{\mathrm{Dose}_{\mathrm{iv}}}{\mathrm{Dose}_{\mathrm{oral}}} \quad (6)$$

By definition, iv bioavailability is assumed to be unity. Because iv doses are normally smaller than oral doses, $\mathrm{AUC}_{\mathrm{oral}}$ is normalized with $\mathrm{AUC}_{\mathrm{iv}}$ by the dose ratio. Because the laws of mass action govern the interaction of a drug with a metabolic enzyme, for many drugs the dose–AUC relationship is not linear. During iv dosing, higher systemic concentrations occur compared to oral dosing because the dose is immediately distributed throughout the volume of distribution. The concentration immediately after an iv dose may saturate the enzymes involved causing disproportionate rise in AUC with dose. In that case, bioavailability could be underpredicted. Chow and Jusko developed a more accurate method of calculating the bioavailability to address this situation [57,58].

Bioavailability calculations are further complicated when different dosage forms are considered. The same dose can show a 3-fold difference in bioavailability depending on the rate of drug release [59,60]. In the case of drug metabolism, the site of release is also important since the distribution of metabolizing enzymes varies along the GI tract. Because of these factors considerable care should be exercised in estimation of bioavailability.

6. Carrier-mediated transport

In order to facilitate absorption of polar nutrients, numerous membrane-bound transport proteins exist in the gastrointestinal tract. Prominent examples include facilitative transporters, the secondary active symporters and antiporters driven by ion gradients, and active ABC (ATP binding cassette) transporters involved in multiple-drug resistance and targeting of antigenic peptides to MHC Class I molecules [61]. Transported substrates range from nutrients and ions to a broad variety of drugs, peptides and proteins. Synthetic conversion of acyclovir to the prodrug Valacyclovir represents one of the most significant examples of enhanced drug absorption due to overlapping transporter specificity between drugs and endogenous substrates. Han et al. found that the prodrugs of two nucleoside analogues increased the intestinal permeability of the parent nucleoside analogue 3- to 10-fold [62]. They also found that dose-dependent permeation enhancement was selective for L-amino acid esters, suggesting stereospecific binding sites on the oligopeptide transporter PepT1 were involved in the enhanced permeation. In addition to transporting its natural substrates, the nutrient di- and tripeptides, PepT1 shows affinity toward a broad range of peptide-like drugs, such as β-lactam antibiotics and angiotensin converting enzyme (ACE) inhibitors [63]. Thus, a combination of passive absorption, gut wall metabolism, carrier-mediated transport, and active efflux make the prediction of bioavailability a complicated problem but one that has tremendous practical benefit in the discovery and design of new drugs.

7. Transport, metabolism, and efflux modeling procedures

While many of these processes – gastrointestinal absorption coupled with efflux and transport, liver metabolism, and pharmacokinetics – have been individually modeled, there is still a need to understand all the processes in tandem. Thus, a mathematical model, which incorporates all the nonlinear processes in a systematic manner, will be invaluable in predicting dose–response relationships, and designing optimum dosage regimens for nonlinearly extracted drugs. We have developed a mathematical model of nonlinear liver and gut metabolism, and nonlinear efflux and influx transport in the gut, and we have incorporated it into the existing advanced compartmental absorption and transit (ACAT) model as implemented in the software package GastroPlus™.

In this study, GastroPlus was used to predict the plasma concentration profiles and bioavailability of drugs subject to nonlinear first pass extraction in the gut and liver and nonlinear efflux and influx transport in the gut. The physico-chemical properties of the drug molecule (solubility, $\log P$), the dosage properties (particle size, particle density, release rate), oral and intravenous plasma concentration profiles, and kinetic constants ($V_{\max}$, K_{m}) were

obtained from literature or were estimated by the computer program QMPRPlus™. Our predictions of bioavailability, fraction absorbed, and plasma concentration profiles were verified for a variety of drugs that undergo: (1) only liver metabolism (propranolol); (2) gut and liver extraction (midazolam); (3) gut efflux (digoxin); and (4) gut efflux and gut and liver metabolism (saquinavir). Good agreement between the observed and simulated C_p vs. time profile was found for all drugs, illustrating the use of in silico methods for clinical studies. The GastroPlus package has also been used to show the sensitivity of the bioavailability and pharmacokinetics of drugs to parameters such as unbound fraction of drug in plasma, metabolic inhibition and induction due to changes in drug–enzyme affinity and enzyme metabolizing capacity, and hepatic blood flow rate. These studies, while providing valuable insight into the individual and synchronous contributions of the different processes, also validate an in silico approach to early drug discovery and design.

7.1. Gastrointestinal drug absorption and elimination model

The ACAT model was modified to include gut wall elimination of drugs by including a series of enterocyte compartments corresponding to each luminal compartment. In this new ACAT model, drug is absorbed from the GI tract by passive diffusion and/or carrier-mediated transport across the apical membrane of the enterocyte. Passive diffusion across the apical membrane (in either direction), driven by the concentration gradient of the drug, follows linear kinetics and is therefore non-saturable, whereas carrier-mediated transport follows Michaelis–Menten kinetics and is saturable. Inside the enterocyte, a saturable efflux process transports drug back into the lumen. Linear, concentration gradient driven, diffusional clearance across the basolateral membrane into or from the blood stream, and saturable metabolism by enzymes all compete to eliminate the drug from the enterocyte compartment.

It is widely believed that the in vivo diffusional resistance to the transfer of drug across the basolateral membrane is much less than that on apical side because of sink conditions created on the basolateral side by systemic blood circulation. Therefore, the intestinal barrier has generally been modeled using the ‘thin wall’ assumption [53]. Contrary to this assumption, it has been observed that some drugs can accumulate in gut wall tissue and the accumulation can significantly alter the rate of drug appearance into circulation as compared to the rate of disappearance from lumen [64]. Based on diffusional resistance from barriers other than the apical membrane of enterocytes, Chiou proposed an ‘absorptive clearance’ model for drug appearance in the systemic circulation [65]. By optimizing plasma profiles of morphine and its metabolite to an absorption model, Cong et al. found that absorptive clearance across the basolateral membrane was greater than that into the intestinal tissue compartment from the lumen [49]. Details of our treatment of the enterocyte volume and basolateral membrane permeability are beyond the scope of this review. Our model of the enterocyte was found to be applicable to all drugs included in this study.

Carrier-mediated transport across the apical membrane of the enterocytes (in either direction) was assumed to follow Michaelis–Menten kinetics. Due to the paucity of experimental data, basolateral transport proteins were not included in the current enterocyte model. It is conceivable that significant concentration gradients exist within the enterocytes as a result of lower diffusion coefficients and protein binding in the cytoplasm. As a first approximation, we assumed that the enterocytes were well mixed and devoid of drug concentration gradient and that binding in the cytoplasm was negligible. Fig. 4 is a schematic of all competing gut, enterocyte and system processes.

7.2. Liver metabolism model

The intestinal absorption model predicts the net rate of disappearance of the drug from the lumen – including transport and efflux – the amount of first pass due to intestinal enzymes, and the rate of appearance of drug in systemic circulation. We used the well-mixed venous equilibrium model to describe the concentration of drug in the liver [66]. Portal venous blood flow transports the absorbed drug into the liver where it mixes with systemic circulation from the hepatic artery containing the drug at its

systemic concentration. The mixing equation which yields the drug liver concentration is given by:

$$C_{liv} = R_{abs}/Q_H + C_p \quad (7)$$

where: C_{liv} is the liver concentration; R_{abs} is the rate of drug absorption from the GI tract which is the sum of the absorption rates from all compartments; Q_H is the hepatic flow rate; and C_p is the plasma concentration.

In the simulations reported here, a standard hepatic blood flow rate of 1500 ml/min was used in the human fasted state, unless information on the hepatic flow rate of the studied subjects was available [67]. Up to a maximum of 100% increase in the hepatic blood flow rate has been reported due to food intake in humans for a short duration [68]. In the simulations reported here, we assumed an average flow 33% greater for the fed state than the fasted rate. Rate of drug elimination from the liver (R_{Metab}) is according to Michaelis–Menten kinetics

$$R_{Metab} = \sum_{i=1}^{n} \frac{V_{max,i} C_{liv}}{(K_{m,i}/f_p + C_{liv})} \quad (8)$$

where: $V_{max,i}$ is the maximum velocity constant of the ith metabolic enzyme; $K_{m,i}$ is the corresponding concentration at which half the maximum velocity is reached; f_p is the fraction of the drug unbound in plasma; and n is the number of enzymes involved in clearing the drug.

The quantity

$$\frac{V_{max}}{\left(\frac{K_m}{f_p} + C_{liv}\right)} \quad (9)$$

can be assumed to be the instantaneous unbound intrinsic clearance (CL_{int}) of the drug from the liver by a particular enzyme.

The total rate of clearance of drug from the liver (CL_h) is given by

$$CL_h = \left(\frac{CL_{int}^{total}}{Q_H + CL_{int}^{total}}\right) Q_H \quad (10)$$

where: CL_{int}^{total} is the sum of the instantaneous intrinsic clearances of all enzymes.

Drug that escapes hepatic extraction is subject to systemic metabolism during subsequent passes through the liver. Therefore, at any instant, a fraction of the drug eliminated by the liver is from systemic circulation and the rest from freshly absorbed drug. Since bioavailability is defined as the fraction of dose that is eliminated before reaching systemic circulation, the amount of freshly absorbed dose that is extracted needs to be estimated. The rate of first pass extraction is simulated by subtracting the metabolism rate based on the systemic concentration (R_{Metab}^{Plasma}) from the total amount metabolized by the liver (R_{Metab}^{Total}). The difference is assumed to correspond to the rate of drug eliminated before reaching systemic circulation (first pass) and hence, it is a measure of the instantaneous bioavailability.

$$\begin{aligned} CL_{int}^{Plasma} &= \frac{V_{max}}{\left(\frac{K_m}{f_p} + C_p\right)} \\ R_{Metab}^{Total} &= CL_{int} C_{liv} \\ R_{Metab}^{Plasma} &= CL_{int}^{Plasma} C_P \\ R_{Metab}^{FirstPass} &= R_{Metab}^{Total} - R_{Metab}^{Plasma} \end{aligned} \quad (11)$$

Michaelis–Menten kinetic constants (V_{max}, K_m) were obtained from in vitro experiments and scaled to in vivo conditions. The intrinsic metabolizing ability of the enzymes, expressed quantitatively by the magnitude of V_{max}, was assumed to depend only on enzyme amounts. Any activity differences between in vitro and in vivo conditions were neglected. For example, if the in vitro V_{max} was reported to be 1 mg/min per mg of microsomal protein, the in vivo V_{max} was calculated using standard values reported in the literature for the mass of microsomal protein in the liver, and total liver mass: 1 mg/min per mg of microsomal protein $\times$ 52.5 mg microsomal protein/g human liver $\times$ 1800 g liver [32].

Scaling of V_{max} based on enzyme amount has been used by other researchers and found to be reasonably accurate in predicting in vivo clearances [39,43]. A similar approach was adopted to describe metabolism in the gut. If the same enzyme is known to metabolize the drug both in the liver and in the gut, the in vitro V_{max} was scaled based on reported amounts of enzymes recovered from each section of the GI tract [46].

In cases where no in vitro enzyme kinetics data were available, a single set of V_{max} and K_m values

was optimized to predict bioavailability and pharmacokinetics of multiple doses or dosage forms using GastroPlus™. The optimized kinetic parameters were then used to assess bioavailability and plasma concentration profiles for different doses of the same drug. Due to lack of in vitro data on enzyme V_{max} and K_m for efflux and transporters, this procedure was adopted in predicting absorption and bioavailability effects for drugs that are actively effluxed or transported in the GI tract.

7.3. Gut metabolism model

Even though the liver is the chief organ of metabolic clearance of drugs in humans, some drugs have been recently recognized as undergoing significant intestinal first pass extraction (e.g. cyclosporine, midazolam). Some P-450 isoforms are present both in the liver and in the intestine, but the liver amounts are 1- to 70-fold higher than the intestinal amounts. It has been postulated that the intestinal first pass is higher than expected from enzyme amounts because in the intestine, all the drug is exposed to the metabolizing enzymes during passage through the enterocytes and the presence of efflux proteins in the enterocytes increases the effective exposure of drugs [46].

The best studied of the P-450 isoforms present in the liver and the intestine is CYP3A4. The amount of 3A4 in the intestine is approximately 70 times less than that in the liver [46,69]. In our simulations, in vitro V_{max} obtained from liver microsomes was scaled to in vivo V_{max} using enzyme-amounts-based scale factors. For example, if the in vitro V_{max} obtained from liver microsomal incubations is V_{liv}, the amount of enzyme in the liver is A_{liv}, and the amount of the same enzyme in a compartment of the GI tract is A_{GIC}, then the V_{max} for biotransformation in the GI compartment V_{GIC} due to the enzyme was calculated as:

$$V_{GIC} = V_{liv} \frac{A_{GIC}}{A_{liv}} \quad (12)$$

7.4. Efflux and transport model

The distribution of P-gp in the human intestine is not well-characterized, though it is widely believed that it is present in all sections of the small intestine and colon [70]. It is also widely believed that the densities increase distally along the GI tract, which would be consistent with increasing biological contamination (metabolic waste products and xenobiotics) along the GI tract. While the existence of P-gp has been proven using in vivo experiments [71], successful in vivo decoupling of passive permeability and active efflux and transport is yet to be successfully achieved. Because physiological factors such as pH (and hence the solubility, log *D* and permeability) and absorptive surface area vary along the GI tract, the decoupling process presents a formidable experimental challenge. Nonetheless, many models have been proposed to explain in vitro saturable efflux [21,72].

To deconvolute a P-gp distribution in the GI tract, we assumed that P-gp was present in the same form and at the same intrinsic activity in all parts of the GI tract. Therefore, any change in the rate of flux in the basolateral to apical direction was only due to changes in the amount of the P-gp present in the compartment. Makhey et al. reported that the efflux ratio, defined as the ratio of the fluxes in the basolateral to apical direction and the apical to basolateral direction, ranged from 1.4 to 19.8 with the highest ratio found in the ileum [70]. We estimated the P-gp amounts in the GI compartments relative to each other on a purely empirical basis with amounts increasing aborally. Because there is limited information available on colon P-gp levels, we assumed similar densities in the colon as in the duodenum.

Under these conditions, for each drug, we optimized one set of efflux V_{max} and K_m values to be used in all simulations. It has been reported that the K_m values of various drugs for P-gp were in the 1–300 μM range [70]. Our optimized values were also in this range. For carrier-mediated transport, the transport proteins (e.g. PepT1) were assumed to be present on the luminal side of the enterocytes. The regional distribution of these transporters is not known; therefore, a constant distribution along the small intestine was assumed. Since very little information is available on basolateral transporters, we neglected basolateral membrane transport. Clearance of drug molecules from the enterocytes into the blood stream was purely by diffusion in our models. For all drugs presented in this study we used a standard ‘log *D*’ model for estimation of the absorption scale factors in each compartment. This very

strict reliance on experimental values limited the number of degrees of freedom in the simulations and allowed us to concentrate on optimization of only a few parameters that illustrated the impact of biochemical and physiological processes on bioavailability.

7.5. Pharmacokinetics modeling

Upon reaching the systemic circulation, a drug is subject to the following processes: (1) distribution to one or multiple peripheral compartments; (2) systemic hepatic clearance; and (3) clearance by the kidney or other clearance organs, including the gut. Parameters for drug distribution to the peripheral compartments were obtained from literature iv data using the PKPlus module of GastroPlus. Based on plasma concentration profiles after an iv dose, PKPlus optimized microconstants (intercompartmental mass transfer rates) and compartmental volumes for one, two, or three-compartment open models. Wherever possible pharmacokinetic parameters were obtained from the same group of subjects used to obtain oral absorption data. Important simplifying assumptions in our pharmacokinetic modeling include linear plasma protein binding, and linear renal and nonhepatic clearances.

7.6. Numerical integration of the model

The resulting set of approximately eighty coupled ordinary differential equations are numerically integrated in GastroPlus™ using a 4th/5th order Runge–Kutta numerical integration scheme with adaptive step-sizing. A 24 h simulation was solved in 1–5 s on a laptop with 600 MHz Pentium III processor. In case of a high degree of nonlinearity arising due to multiple competing saturable processes, the numerical integrator took up to 20 s for some simulations on the same computer.

8. Results of selected simulations

8.1. Hepatically eliminated drugs (propranolol)

Propranolol is a widely used β-adrenoceptor blocking agent. The conjugate acid form of propranolol is highly soluble in the pH range that exists in the GI tract and it is also rapidly and completely absorbed from the proximal small intestine. Due to high hepatic clearance, the plasma half-life is short – varying from 1.5 to 3 h [73,74]. After administration of single oral doses, hepatic extraction remains high and much of the dose is eliminated from hepatic portal blood during transfer from the gut, so that little drug reaches the systemic circulation [73]. Intestinal and renal clearances are negligible. Bioavailability of propranolol is highly variable in humans (20–70%) [31,59,75]. Hepatic extraction is also responsible for nonlinear dose–response relationships in the therapeutic dosage range [59,76]. With continued administration, the avid removal process becomes saturated, extraction ratio falls, and propranolol accumulates approximately 2-fold. Drug $t_{1/2}$ is prolonged to 3–6 h under these conditions. The pharmacokinetics of propranolol vary according to the route and duration of administration. After iv administration, the decline in drug concentrations is biphasic and the drug is cleared very efficiently by the liver, so that its elimination is dependent largely on liver blood flow [77,78]. Propranolol is also highly bound to plasma protein (~90%) [76], though convincing evidence regarding nonlinearity of the binding process is not yet forthcoming.

As many as 29 metabolites of propranolol have been recovered in urine after oral administration [74]. While in vitro kinetic constants of substrate clearances are not available, many researchers have estimated V_{max} and K_m values based on mathematical models (e.g. Refs. [75,76]). Because of its high clearance, nonlinear dose–response relationship, highly variable hepatic clearance, and high protein binding, many models have been proposed to explain propranolol pharmacokinetics and to design extended release dosage forms.

Using the PKPlus™ module of GastroPlus, we fitted one, two, and three-compartment pharmacokinetic parameters to the average plasma concentration profile for six fed subjects who were administered an iv infusion of 8.2 mg of propranolol over 8.2 min [79]. The two-compartment fit was selected on the basis of having the lowest value for the Akaike Information Criterion. A single set of enzyme kinetic constants was optimized to fit the average oral plasma concentration profile for administration of both an immediate release (conventional film-coated tablet) and an extended release

formulation (noted as F1 in McAinsh Fig. 1) [60]. The optimized V_{max} value was 0.045 mg/s (3888 mg/day) and true K_m was 0.05 μg/ml at a plasma unbound fraction of 9% (apparent $K_m = 0.55$ μg/ml) (Fig. 5).

Nonlinear dose–response relationships were predicted in the dosage range 40–200 mg (5-fold increase) with a simulated 8.4-fold increase in C_{max}. Parameter sensitivity analysis simulations revealed that the systemic clearance of propranolol was found to increase with increasing hepatic flow rate and AUC, consequently, decreased by 31% for a 4-fold increase in hepatic blood flow ($Q_H = 0.75–3.0$ l/min). The fraction of the dose (160 mg of HCl salt) bioavailable increased with the same increase in hepatic flow rate resulting in a simulated increase in bioavailability from 34 to 53%. This somewhat unusual behavior (decreasing AUC when bioavailability increases) is caused by a reduction in first pass extraction at higher Q_H, coupled with an increase in the rate of systemic clearance due to the higher Q_H. An increase in the unbound fraction of propranolol in plasma resulted in a predicted decrease in the AUC, C_{max}, and bioavailability.

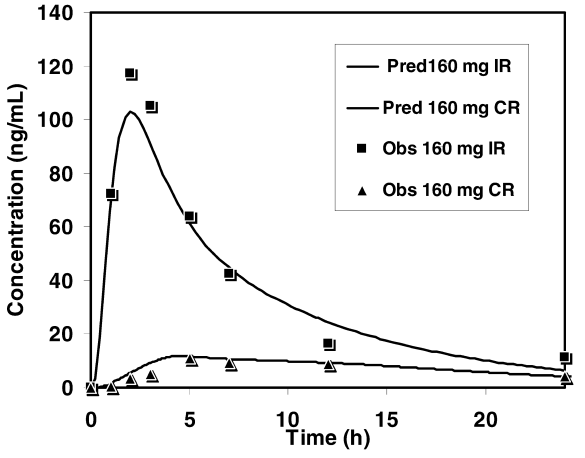

Fig. 5. Predicted and observed plasma concentration profiles for a 160 mg immediate release (IR) and extended release (ER) dose of propranolol [60]. Pharmacokinetic parameters were obtained by fitting an average iv C_p–time profile to a two compartment pharmacokinetic model. Optimized V_{max} (=0.045 mg/s) and K_m (=0.05 mg/l) for liver P-450 metabolism were used in these predictions. Bioavailability for the fully absorbed IR dose was 43% while only 53% of the ER dose was absorbed in 48 h and 13% of the dose was bioavailable.

8.2. Drugs undergoing hepatic and intestinal biotransformation (midazolam)

Midazolam is a short-acting benzodiazepine with anxiolytic, sedative-hypnotic and marked amnestic properties. In spite of its rapid absorption from the small intestine, it has a low in vivo bioavailability due to extensive hepatic and intestinal extraction [80,81]. Using in vivo probes such as grapefruit juice (GFJ), which is a potent inhibitor of 3A4 activity in the small intestine but not the liver, the fraction of midazolam extracted in the intestine and liver has been studied [82]. Pharmacokinetic studies on patients in the anhepatic phase of liver transplant operations also revealed interesting insights into site-dependent metabolism of midazolam [22,83]. Paine et al. found the intestinal extraction to be 44% and the hepatic extraction to be 43% of the amount entering the portal vein with an overall oral bioavailability of 30% [22]. Tsunoda et al. found the total extraction in the gut to be 48% with 40% of the remaining drug extracted by the liver producing a net bioavailability of 29% [83]. Thus, the first pass extraction by liver in these two cases would be approximately 24% and 21% of the total drug, respectively. It was also found that a much smaller fraction (8%) of the drug was extracted during each pass across the splanchnic bed after intravenous administration, demonstrating route-dependent intestinal metabolism, but also demonstrating that even for iv doses, gut metabolism can be significant. In vitro enzyme kinetic constants have been determined by incubating midazolam with microsomal preparations [84,85].

Based on literature and in silico biopharmaceutical parameters predicted from QMPRPlus, and PKPlus-fitted pharmacokinetic parameters, we predicted fraction absorbed, first pass extraction in the intestine and liver, bioavailabilities, and the plasma-concentration profiles for six different p.o. doses of midazolam and one iv dose. These doses included 15 mg p.o. doses administered with and without grapefruit juice [82] (Fig. 6), 7.5, 15 and 30 mg p.o. solutions [86] (Fig. 7), 2 mg intraduodenal dose during the anhepatic phase of a liver transplant operation, and a 5 mg iv bolus (not shown) [82]. The metabolic enzyme kinetic constants were obtained from in vitro experiments on liver and intestinal

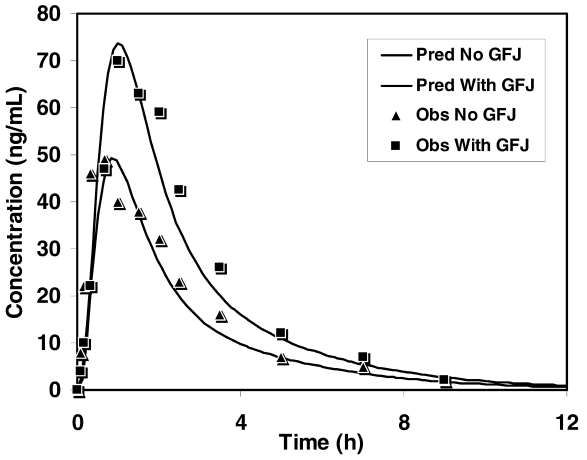

Fig. 6. Midazolam administration with and without grapefruit juice (GFJ) treatment [82]. In this study 15 mg of midazolam (tablet) was administered to eight male subjects (average weight = 82 kg) before and after consumption of two glasses (200 ml each) of GFJ 1 h before administration. QMPRPlus was used to estimate human effective permeability (12×10^{-4} cm/s), pure aqueous water solubility (8.76 μg/ml), and log *P* (3.86). The metabolic enzyme kinetic constants were obtained from in vitro experiments on liver and intestinal microsomes ($V_{max}=0.44$ mg/s, $K_m=1.21$ mg/l) [46]. After GFJ treatment, the oral bioavailability was observed to increase by 33% relative to dose administered without GFJ.

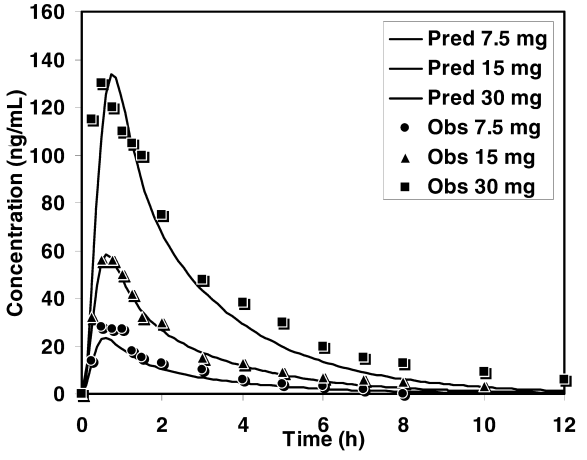

Fig. 7. Nonlinear kinetics of midazolam [86]. The same biopharmaceutical properties were used in these simulations as described in Fig. 6. However, since these were different subjects, a new set of two compartment pharmacokinetic parameters was optimized over all three doses simultaneously. As the dose is increased by a factor of 4 (7.5–30 mg), bioavailability increased from 25 to 38% in our predictions.

microsomes ($V_{max}=0.44$ mg/s, $K_m=1.21$ mg/l) [46]. A standard hepatic flow rate of 1500 ml/min and 96% plasma protein binding was assumed. Volume of distribution, and transfer rate constants for a two compartment pharmacokinetic model were determined from the average C_p vs. time profile of a 5 mg iv bolus administration in eight male subjects who received both the 15 mg p.o. and 5 mg iv doses. A separate set of pharmacokinetic parameters was fitted to the data for the three solution formulations [86].

The predicted bioavailability of the p.o. 15 mg dose of midazolam taken without grapefruit juice was 28% and it increased to 44% when administered with grapefruit juice. Significant extraction was predicted for both the gut (55%) and liver (45%) when midazolam was administered without GFJ. In the case of midazolam administered with GFJ, it was observed that the gut metabolism V_{max} had to be reduced by 62% to predict the plasma concentration profiles. For the anhepatic intraduodenal dose, it was predicted that 70% of the dose was extracted in the gut. Midazolam exhibited nonlinear kinetics in the dosing range 7.5 mg–30 mg. The predicted bioavailability increased from 25% for the 7.5 mg dose to 38% for the 30 mg dose with a 6-fold increase in C_{max}. For the iv bolus, it was predicted that approximately 1% of the dose was extracted in the intestine and the rest in the liver.

8.3. Drugs effluxed in the gut (Digoxin)

About 70–80% of an oral dose of digoxin is absorbed, mainly in the proximal part of the small intestine [87,88]. The degree of binding to serum albumin is 20–30%. Digoxin is extensively distributed in the tissues, as reflected by the large volume of distribution. Nearly all of the digoxin in urine is excreted unchanged, with a small part as active metabolites [89]. About 25–28% of digoxin is eliminated by nonrenal routes, primarily in the feces. This is widely believed to be due to exsorption of the drug from the gut wall enterocytes due to gut P-gp [90,91]. Greiner et al. found that approximately 10% of the clearance of a 1 mg iv dose of digoxin was found to be non-renal. Oral bioavailability of digoxin was found to decrease when administered after rifampin treatment, and increase when administered

with quinidine. Rifampin is a known inducer of gut (but not renal) P-gp and quinidine is a known inhibitor of both intestinal and renal P-gp [90].

Using a three compartment model, the pharmacokinetics for the 1 mg iv dose was determined. From the fitted clearance of 0.33 l/h per kg, we assumed 90% of the total oral clearance to be renal (0.29 l/h per kg). We then optimized P-gp efflux V_{max} and K_m kinetic constants based on the iv plasma concentration profile to account for the additional 10% of the total clearance. The optimized constants for digoxin were found to be 0.009 mg/s and 4 mg/l. Based on the assumed P-gp distribution in the GI tract, and optimized V_{max} and K_m for substrate P-gp interactions, plasma concentration profiles and bioavailabilities were obtained for oral digoxin administered alone and after rifampin treatment. Greiner et al. found that after rifampin treatment, in duodenal biopsies, P-gp expression was increased by 3.5-fold. In our simulations, a 2.5-fold increase in the V_{max} of the intestinal P-gp was required to match the plasma concentrations and bioavailabilities. The predicted oral bioavailability over 24 h was reduced by approximately 41% with rifampin treatment (66–39%). For the iv control dose, it was predicted that 92% of the dose was eliminated renally over 48 h and the other 8% was exsorbed into the lumen and excreted in feces. With rifampin treatment, the predicted cumulative renal excretion amount decreased to 87%. For the oral dose, the cumulative renal excretion amount decreased by 41% due to rifampin treatment.

8.4. Drugs metabolized and effluxed in the gut (Saquinavir)

Saquinavir was the first clinically available HIV protease inhibitor in the USA. It has a very low bioavailability (0.5–2%) due to extensive first pass metabolism by CYP3A4 in the gut and in the liver. It is also a gut P-gp substrate [92,93]. The bioavailability of saquinavir was found to double when administered with food or with grapefruit juice. The interaction has been attributed to increased hepatic blood flow due to food intake and suppression of intestinal 3A4 and P-gp by grapefruit juice respectively [94,95]. During oral administration of saquinavir, a second peak is observed approximately 5 h after administration. This peak has been attributed to food effects. When grapefruit juice was added iv plasma concentration profiles did not change significantly. In vitro incubation of saquinavir with hepatic and intestinal microsomes resulted in similar product distribution due to enzymatic oxidation with two main metabolic products [96,97]. The high intrinsic clearance of saquinavir suggests that mesenteric mucosal and hepatic blood flow rates are the limiting factors in its clearance.

The biopharmaceutical properties of saquinavir were estimated using the software package QMPRPlus. An open three compartment pharmacokinetic model best fit the iv data by PKPlus. The kinetic constants, V_{max} and K_m, for P-gp efflux were optimized to fit the data and were found to be 0.009 mg/s and 10 mg/l, respectively. The value for K_m was set to an arbitrarily high value to ensure that there would not be saturation of P-gp and the V_{max} was optimized to explain the C_p vs. time profile. In vitro kinetic constants ($V_{max}=4.24$ mg/s, $K_m=0.27$ mg/l, [96]) were used for both gut and liver metabolism and the V_{max}'s were scaled according to the amounts of 3A4 in the small intestine and liver as described earlier. Plasma protein binding was assumed to be 97% [98]. It was estimated that approximately 81% of a 600 mg dose of saquinavir was absorbed from the GI tract in 24 h and 0.56% of the dose was bioavailable (Fig. 8). Our simulations show that solubility was an important factor in the oral absorption of saquinavir. We found that the second peak in the plasma concentration curve could be affected by increased dissolution rate of saquinavir in the slightly more acidic environment of the colon compared to ileum (Fig. 9) and by the regional distribution and V_{max} of P-gp. Due to these factors, significant colon absorption (~20%) was predicted. When saquinavir was taken with GFJ, the bioavailability increased to 0.93% in 24 h, while a similar fraction of the dose was absorbed. In the presence of GFJ, gut metabolism was estimated to contribute approximately 51% of the total first pass and 63% in the absence of GFJ. For saquinavir taken with GFJ, the V_{max} for gut metabolism was scaled down by a factor of 30% and efflux V_{max} had to be scaled down by 22% to match the observed plasma concentration profiles.

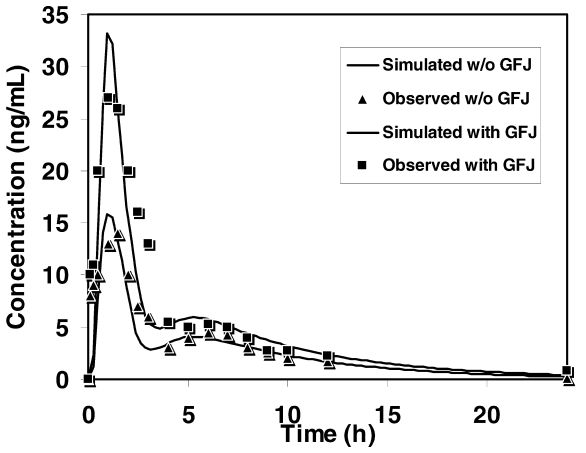

Fig. 8. Oral bioavailability of saquinavir with and without GFJ [95]. In this study 600 mg of saquinavir (three capsules of Invirase 200 mg each tablet) was administered to eight healthy male subjects (average weight = 76 kg) before and after consumption of two glasses (200 ml each) of GFJ at 15 and 45 min prior to administration. QMPRPlus was used to estimate human effective permeability (0.93×10^{-4} cm/s), pure aqueous water solubility (57.1 μg/ml), and log *P* (3.7). The metabolic enzyme kinetic constants were obtained from in vitro experiments on liver and intestinal microsomes (V_{max} = 4.24 mg/s, K_m = 0.27 mg/l) [96]. The kinetic constants, V_{max} and K_m, for P-gp efflux were optimized to fit the data and were found to be 0.009 mg/s and 10 mg/l, respectively. After GFJ treatment, the oral bioavailability was observed to double.

9. Discussion

9.1. Liver metabolism

Based on literature biopharmaceutical properties and optimized liver V_{max} and K_m, we predicted the plasma concentration profile, fraction absorbed, and the bioavailability of two different doses of propranolol (IR and ER doses). The predicted quantities agreed well with literature values. Based on steady state plasma concentrations, Wagner et al. [75] estimated a pooled V_{max} of approximately 450 mg/day and an apparent K_m of 0.05 mg/l [75] while our estimates were 3888 mg/day and 0.05 mg/l (true K_m) respectively. The difference between the V_{max} estimates might be due to the fact that Wagner et al. used steady state concentrations and dose–independent equations to estimate their kinetic constants. Another contribution to the discrepancy could be that they assumed a hepatic extraction model unlimited by blood flow. In our model, even though the intrinsic clearance is much higher (due to higher V_{max} values), the overall clearance is limited by the hepatic flow rate. Von Buhr reported K_m values in the range of 5–50 μM (1–10 mg/l) from in vitro incubations of propranolol with dog liver microsomes [99]. Since propranolol is highly bound to plasma proteins (~90%), the apparent in vivo K_m is an order higher (10–100 mg/l). If this were indeed true, nonlinear dose–response relationships would be seen only when in vivo concentrations approach the in vivo K_m. For a 140 mg dose of propranolol, an in vivo C_{max} of 0.12 mg/l was observed and nonlinear dose–C_{max} relationship was observed in the range 40–320 mg [100]. Therefore, the true in vivo K_m would need to be in the range of 0.01–0.1 mg/l for nonlinearity to be observed in the above-mentioned dose range. Also, for propranolol, it has been suggested that the hepatic removal is so avid that both bound and unbound fractions are simultaneously eliminated [73]. This is contrary to our assumption that only unbound drug is available for hepatic removal and would serve to explain the discrepancy in our optimized kinetic constants. Under linear conditions, the optimized V_{max} and K_m values yield a total hepatic clearance of approximately 80 l/h (Eq. (10)). The reported range of propranolol clearance from iv doses is 60–80 l/h [78,100].

Our predictions of plasma concentration profiles agreed well with those reported in literature [60]. Although the bioavailability in the set of volunteers used in this study was not reported, bioavailabilities of a 160 mg dose have been reported to be in the range 18–60% [101]. Nonlinear dose–response relationships of propranolol have been well characterized with an 8-fold increase in dose (40–320 mg) causing more than a 14-fold increase in C_{max} (18–252 ng/ml) [100].

Food has been known to have a profound effect on the bioavailability of propranolol with a reported 19% increase in bioavailability (27–46%) due to food intake associated with a 34% increase in hepatic flow rate [79]. Post-prandial increase in hepatic blood flow has been estimated at up to two-times that in the fasted state [68]. This effect is presumably temporary with the flow returning to the normal fasted-state rate in a few hours. Since the duration of increase is not well known, in our simulations, we

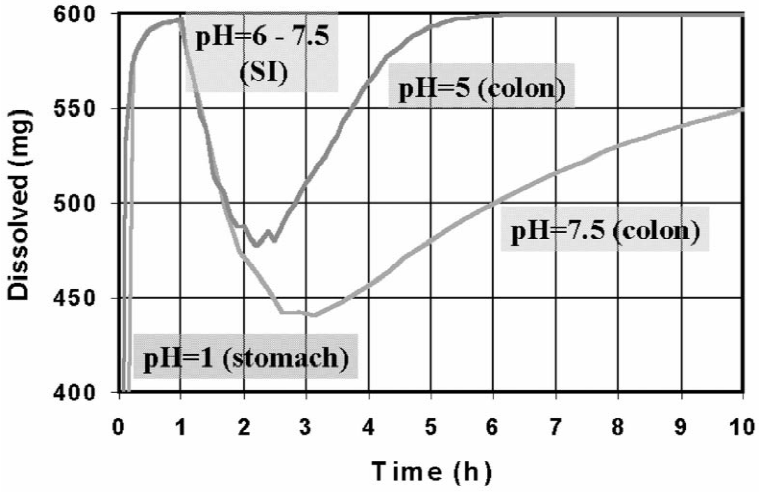

Fig. 9. Dissolution of saquinavir in the GI tract. Two cases, corresponding to limiting colon pHs of 5 and 7.5 are shown to illustrate simulation of dissolution for. Since saquinavir solubility decreases with increasing pH (from 1 to 8), precipitation occurs as the drug enters the small intestine (shown by the decreasing amount dissolved curve). When the drug enters the colon at pH = 5, increased dissolution contributes to the second peak. When the colon pH is simulated at a value of 7.5, dissolution is appears to be slower, but increased permeability (due to increased log *D*) might be expected to cause increased absorption.

used an average increase of 34% in the hepatic flow rate and maintained the flow rate for the entire duration of the simulation [76]. Our simulation showed that the increased hepatic flow rate caused an increase in the bioavailability from 41 to 46% (not shown) while the oral AUC decreased slightly. While the bioavailability increase was not as dramatic as that reported, an average increase in the flow rate was assumed in our case and the effect of the meal contents on the protein binding of propranolol was also neglected. Significant and insignificant changes in the AUC of propranolol have been observed when administered with food [100].

9.2. Gut metabolism

Gut metabolism is more difficult to characterize than liver metabolism because of limited experimental data on the distribution of enzymes in the different regions of the GI tract. The present study involves the two best characterized gut enzymes, 3A4 and 2D6. Intestinal distribution for these enzymes were obtained from the literature and used in our simulations as described earlier (Section 7.3).

Midazolam has been well characterized with respect to its intestinal first pass. In the anhepatic phase of liver transplant operation, 43% of the administered oral midazolam was found to be bioavailable [22]. We predicted 30% bioavailable (not shown). In spite of 70-fold higher amounts of 3A4 in the liver than in the intestine [33], Paine found that the unbound intrinsic clearance of midazolam by liver and intestinal microsomes was similar. Therefore, they surmised that cytosolic protein binding might not be an important factor in intestinal metabolism of midazolam, while plasma protein binding would be an important factor for liver metabolism. GFJ is known to increase oral bioavailability of some drugs by suppression of P-gp and 3A4 expression [102]. Since midazolam is not a P-gp substrate, it is generally agreed that an increase in the bioavailability due to GFJ is solely due to suppression of intestinal first pass since liver 3A4 expression is not affected by grapefruit juice. We found that the 3A4 V_{max} for gut metabolism of midazolam had to be reduced by 62% to simulate the data from the Kupferschmidt study [82]. Lown et al. studied both the protein amounts and the mRNA expression of CYP-3A4 responsible for the increase in felodipine oral bioavailability due to grapefruit juice [103]. They observed that the concentration of CYP3A4 in small bowel epithelia (enterocytes) fell 62% with no

corresponding change in CYP3A4 mRNA levels after consumption of grapefruit juice. In addition, enterocyte concentrations of CYP3A4 measured before grapefruit juice consumption correlated with the increase in C_{max} when felodipine was taken with either the 1st or the 16th glass of grapefruit juice relative to water. Therefore, our observation that GFJ reduces intestinal 3A4 activity for midazolam metabolism by 62% is in excellent agreement. Paine et al. found that from an intravenous dose of 1 mg, the time-averaged fraction of midazolam extracted by intestinal mucosa and other viscera drained by the hepatic portal vein was 8%. In our simulations, we predicted that approximately 1% of the total iv dose was extracted due to intestinal metabolism. This underprediction might be due to the assumption in our model that the splanchnic bed is perfused by the entire hepatic flow rate. In reality, only a portion of this flow is exposed to the intestinal enzymes [48,49]. This lower perfusion rate might cause a higher exposure of the drug to the metabolizing enzymes and thus cause a higher fraction to be extracted.

The route-dependence of intestinal metabolism is also governed by the residence time of the drug in the enterocytes that house the 3A4 enzymes. The residence time can be increased because of binding in the cytoplasm, presence of effluxers in the enterocytes, limited villous blood flow, and decreased by factors such as high basolateral clearance and basolateral transporters. We found through our simulations that the basolateral transfer rate was an important determinant in the amount of the exposure of the drug to the metabolizing enzymes in the enterocytes.

The in vivo enzyme regional distribution form another important factor in the amount of first pass since the site of metabolism is dependent on the site of absorption (and hence the dissolution). Since up to 30-fold variations in 3A4 expression in the small intestine have been reported [45,104], care should be taken in making average clinical decisions based on specific groups of individuals. Due to region-specific changes in 3A4 expression, and route-dependent intestinal first pass, ER doses can be designed to increase drug bioavailability by avoiding sites of high intestinal first pass. For example, for a drug that is well absorbed from the colon and is a 3A4 substrate, delayed release of drug material will ensure that higher amounts of drug will reach the systemic circulation (as long as it is not a substrate for efflux proteins). As more experimental information on other metabolizing enzymes becomes available, a wider variety of drugs could be studied to evaluate their intestinal first pass.

Using a similar approach to the P-450 isoform 2D6, which metabolizes metoprolol, we found that approximately 1.4% of a 160 mg dose of metoprolol was metabolized in the gut and about 48% in the liver. Madani et al. predicted 0.8% metabolized in the gut, which agrees well with literature bioavailabilities of metoprolol [105].

9.3. Efflux and transport

As mentioned earlier, saturable efflux and transport are processes that are difficult to distinguish from passive diffusion in the small intestine. Changes in physiological conditions such as pH in the GI tract affect the transcellular and paracellular components of a drug's effective permeability. Ideally, these changes need to be accounted for before carrier-mediated transport can be independently estimated and correlated with the amount of the carrier present in the region of the tissue. Makhey et al. used etoposide as a probe to evaluate regional dependence of P-gp efflux in the human GI tract and obtained ratios of basolateral to apical/apical to basolateral (BA/AB) fluxes in the duodenum, ileum, and colon [70]. In the absence of information regarding changes in the passive permeability of etoposide under changing pH conditions that exist in the GI tract, we assumed that any change in net transport of the drug across the membrane was entirely due to differences in P-gp content and determined the relative amounts of P-gp in the different compartments of the GI tract. Since we are not aware of any studies where P-gp amounts have been quantitatively determined in different parts of the small intestine, the accuracy of the assumed density distribution of P-gp in the small intestine was not verifiable.

Rifampin has been found to induce P-gp to a considerable extent [106]. Grenier et al. reported a 3.5-fold increase in P-gp expression in the duodenum after 7 days of rifampin treatment [90]. Our predicted increase of V_{max} by a factor of 2.5 for the

efflux of digoxin (a non-metabolized cardiac glycoside) parallels the experimental observation. The slight difference could be due to errors in our assumed P-gp distribution and the consequent errors in the optimized kinetic constants. It could also be that the degree of expression of P-gp in other sections of the small intestine did not vary as much as it did in the duodenum. From an iv dose of digoxin, Greiner et al. observed that approximately 10% of the total clearance occurred through non-renal routes (presumably due to P-gp efflux and elimination in the feces). After rifampin treatment, Greiner et al. found that the non-renal clearance increased 3-fold while the renal clearance remained the same. In our predictions, using optimized efflux V_{max} and K_m values, 8% of the control iv dose was eliminated in feces. With rifampin treatment, a 62% increase in exsorptive clearance (to 13%) was observed. While our predictions are slightly below the experimental observations, more experimental data on P-gp distribution in the GI tract is required before clinically significant predictions can be made. It would be possible to fit the observed plasma concentration data for digoxin by optimizing the V_{max}, K_m, and the P-gp distribution scale factors; however, we felt that with the limited data available, such an approach would not be appropriate.

For saquinavir in our simulations, a significant (~63%) amount of the drug was metabolized during first pass through the small intestine. Hitherto, gut and liver first pass of saquinavir have not been separately estimated. Our simulations show that inhibition of gut first pass will have significant impact on the overall bioavailability of saquinavir. Experimentally, this has been observed [93–95] where bioavailability doubled when saquinavir was administered with grapefruit juice or increased 30-fold when administered with ritonavir. If we assume that ritonavir completely inhibits gut metabolism and gut efflux, we predict a 6-fold increase in the AUC of saquinavir when it is administered with ritonavir (not shown). Since a 50-fold increase in AUC is seen with concomitant ritonavir administration [97], hepatic elimination is probably also inhibited to a significant extent by ritonavir. Our simulation gives a 50-fold increase in AUC when hepatic elimination is decreased by 88%. The fraction of the dose absorbed was simulated to be lesser by 17% in the case where gut metabolism was fully inhibited while bioavailability was increased approximately 4-fold. In this case, since intestinal metabolism was absent, efflux, which is a competing process, was the chief means by which drug bioavailability was reduced. Since effluxed drug returns to the lumen, a lower fraction absorbed was predicted.

Although a reduction of CYP3A4 by 62% in the presence of GFJ was able to explain the C_p vs. time profile for midazolam, we found that a 30% reduction was all that was needed to explain the data for saquinavir. Based on the available data, we cannot conclude that the smaller predicted effect of GFJ in the saquinavir studies was due to patient physiology or an effect that is specific to each CYP3A4 substrate.

It is widely believed that the second peak in the plasma concentration is due to increased hepatic flow rate caused by food intake. Our simulations show that it could also be due to dissolution characteristics of saquinavir in colon. Since saquinavir has an ionizable group, a weak base at $pK_a = 7.35$, more of the drug exists in the neutral form as pH increases along the small intestine. At the lower pH's that exist in the caecum, ionization increases thus increasing solubility and dissolution, resulting in increased absorption. However, the appearance of the second peak in plasma concentration was also dependent on both the effective permeability and the density of P-gp in the colon. For most lipophilic drugs, it is generally assumed that the colon permeability is equal to or higher than that in the small intestine (e.g. metoprolol, propranolol, [27]. With such permeability, the second peak arises due to increased solubility and dissolution. However, since the colonic permeability of saquinavir has not been characterized in vivo, and the amount of P-gp in colon also is not well-characterized, it is impossible to conclusively say whether the second peak is related to solubility/dissolution, permeability, or efflux.

10. Conclusions

1. We have developed a new model of saturable processes in oral drug absorption that simulates nonlinear responses in drug bioavailability and pharmacokinetics.

2. We have validated the model against experimental data for drugs that undergo liver metabolism alone, gut metabolism and liver metabolism, and efflux and metabolism.
3. We used in vitro kinetic constants obtained from homogenate or whole cell experiments under controlled conditions and scaled the constants to the in vivo scenario using appropriate physiological scale factors. Our results show that in vitro kinetic constants can be used to predict drug behavior in vivo provided adequate data on enzyme distribution and activity are available. Factors such as interindividual variability in enzyme content and activity strongly limit extension of predictions across different demographics.
4. More experimental information is needed regarding distribution and densities of metabolizing enzymes and efflux proteins in the GI tract. This information is crucial since dissolution and absorption are site-dependent all along the GI tract. Variation in enzyme and efflux transporter amounts in the intestine and colon can also be utilized to design formulations with increased bioavailabilities by avoiding sites of high intestinal first pass and efflux.
5. Influence of inhibitors and inducers of enzymes can be modeled using appropriate scale factors to mimic changes in enzyme amounts, activity, and competitive inhibition.
6. For drugs that are substrates of both efflux proteins and metabolic enzymes in the small intestine, these proteins work in tandem in reducing or increasing the oral bioavailability of drugs.

The above-described mathematical model has its limitations, such as the assumption of the venous equilibrium model for hepatic elimination. For highly extracted drugs, the venous equilibrium model predicts different fraction extracted in the liver than the parallel-tube or dispersion models. Therefore, provisions for using other models may enhance the predictability of the simulation. A more complete characterization of gut enterocytes, the underlying gut tissue, and cytoplasmic protein binding would allow an even more comprehensive absorption model. Segregation of the blood flow to the intestine might better explain route-dependent intestinal metabolism.

In spite of its limitations, the ACAT model combined with modeling of saturable processes has the potential to become a powerful tool in the study of oral absorption and pharmacokinetics. To our knowledge, it is the only tool that can translate in vitro data from early drug discovery experiments all the way to plasma concentration profiles and nonlinear dose-relationship predictions. As more experimental data becomes available, we believe that the model will become more comprehensive and its predictive capabilities will be further enhanced.

Acknowledgements

We gratefully acknowledge the work of Robert Fraczkiewicz, Grace Fraczkiewicz, and Boyd Steere who helped to collect literature data and developed the application QMPRPlus™ used for estimation of some of the biopharmaceutical properties in this article.

References

[1] S.D. Hall, K.E. Thummel, P.B. Watkins, K.S. Lown, L.Z. Benet, M.F. Paine, R.R. Mayo, D.K. Turgeon, D.G. Bailey, R.J. Fontana, S.A. Wrighton, Molecular and physical mechanisms of first-pass extraction, Drug. Metab. Dispos. 27 (1999) 161–166.
[2] L.X. Yu, E. Lipka, J.R. Crison, G.L. Amidon, Transport approaches to the biopharmaceutical design of oral drug delivery system: prediction of intestinal absorption, Adv. Drug Deliv. Rev. 19 (1996) 359–376.
[3] M.H. Jacobs, Some aspects of cell permeability to weak electrolytes, Cold Spring Harbor Symp. Quant. Biol. 8 (1940) 30–39.
[4] C.A.M. Hogben, D.J. Tocco, B.B. Brodie, L.S. Schanker, On the mechanism of intestinal absorption of drugs, J. Pharmacol. Exp. Ther. 125 (1959) 275–282.
[5] A. Suzuki, W.I. Higuchi, N.F. Ho, Theoretical model studies of drug absorption and transport in the gastrointestinal tract II, J. Pharm. Sci. 59 (1970) 651–659.
[6] A. Suzuki, W.I. Higuchi, N.F. Ho, Theoretical model studies of drug absorption and transport in the gastrointestinal tract I, J. Pharm. Sci. 59 (1970) 644–651.
[7] N.F. Ho, W.I. Higuchi, J. Turi, Theoretical model studies of drug absorption and transport in the GI tract (3), J. Pharm. Sci. 61 (1972) 192–197.
[8] N.F. Ho, W.I. Higuchi, Quantitative interpretation of in vivo buccal absorption of n-alkanoic acids by the physical model approach, J. Pharm. Sci. 60 (1971) 537–541.

[9] J.B. Dressman, D. Fleisher, G.L. Amidon, Physicochemical model for dose-dependent drug absorption, J. Pharm. Sci. 73 (1984) 1274–1279.
[10] A.B. Suttle, G.M. Pollack, K.L. Brouwer, Use of a pharmacokinetic model incorporating discontinuous gastrointestinal absorption to examine the occurrence of double peaks in oral concentration–time profiles, Pharm. Res. 9 (1992) 350–356.
[11] J.D. Wright, T. Ma, C.K. Chu, F.D. Boudinot, Discontinuous oral absorption pharmacokinetic model and bioavailability of 1-(2-fluoro-5-methyl-beta-L-arabinofuranosyl)uracil (L-FMAU) in rats, Biopharm. Drug Dispos. 17 (1996) 197–207.
[12] D.A. Norris, G.D. Leesman, P.J. Sinko, G.M. Grass, Development of predictive pharmacokinetic simulation models for drug discovery, J. Controlled Release 65 (2000) 55–62.
[13] L.X. Yu, J.R. Crison, G.L. Amidon, Compartmental transit and dispersion model analysis of small intestinal transit flow in humans, Int. J. Pharm. 140 (1996) 111–118.
[14] L.X. Yu, G.L. Amidon, A compartmental absorption and transit model for estimating oral drug absorption, Int. J. Pharm. 186 (1999) 119–125.
[15] P.J. Sinko, G.D. Leesman, G.L. Amidon, Predicting fraction dose absorbed in humans using a macroscopic mass balance approach, Pharm. Res. 8 (1991) 979–988.
[16] D.M. Oh, R.L. Curl, G.L. Amidon, Estimating the fraction dose absorbed from suspensions of poorly soluble compounds in humans: a mathematical model, Pharm. Res. 10 (1993) 264–270.
[17] T. Sawamoto, S. Haruta, Y. Kurosaki, K. Higaki, T. Kimura, Prediction of the plasma concentration profiles of orally administered drugs in rats on the basis of gastrointestinal transit kinetics and absorbability, J. Pharm. Pharmacol. 49 (1997) 450–457.
[18] A. Kalampokis, P. Argyrakis, P. Macheras, A heterogeneous tube model of intestinal drug absorption based on probabilistic concepts, Pharm. Res. 16 (1999) 1764–1769.
[19] A. Kalampokis, P. Argyrakis, P. Macheras, Heterogeneous tube model for the study of small intestinal transit flow, Pharm. Res. 16 (1999) 87–91.
[20] B.R. Stoll, R.P. Batycky, H.R. Leipold, S. Milstein, D.A. Edwards, A theory of molecular absorption from the small intestine, Chem. Eng. Sci. 55 (2000) 473–489.
[21] K. Ito, H. Kusuhara, Y. Sugiyama, Effects of intestinal CYP3A4 and P-glycoprotein on oral drug absorption-theoretical approach, Pharm. Res. 16 (1999) 225–231.
[22] M.F. Paine, D.D. Shen, K.L. Kunze, J.D. Perkins, C.L. Marsh, J.P. McVicar, D.M. Barr, B.S. Gillies, K.E. Thummel, First-pass metabolism of midazolam by the human intestine, Clin. Pharmacol. Ther. 60 (1996) 14–24.
[23] K. Arimori, M. Nakano, Drug exsorption from blood into the gastrointestinal tract, Pharm. Res. 15 (1998) 371–376.
[24] K. Arimori, M. Nakano, The intestinal dialysis of intravenously administered phenytoin by oral activated charcoal in rats, J. Pharmacobiodyn. 10 (1987) 157–165.
[25] W.H. Press, Numerical recipes in C: the art of scientific computing, Cambridge University Press, Cambridge, New York, 1992.
[26] V. Pade, S. Stavchansky, Estimation of the relative contribution of the transcellular and paracellular pathway to the transport of passively absorbed drugs in the Caco-2 cell culture model, Pharm. Res. 14 (1997) 1210–1215.
[27] A.L. Ungell, S. Nylander, S. Bergstrand, A. Sjoberg, H. Lennernas, Membrane transport of drugs in different regions of the intestinal tract of the rat, J. Pharm. Sci. 87 (1998) 360–366.
[28] A. Adson, P.S. Burton, T.J. Raub, C.L. Barsuhn, K.L. Audus, N.F. Ho, Passive diffusion of weak organic electrolytes across Caco-2 cell monolayers: uncoupling the contributions of hydrodynamic, transcellular, and paracellular barriers, J. Pharm. Sci. 84 (1995) 1197–1204.
[29] S.M. Pond, T.N. Tozer, First-pass elimination. Basic concepts and clinical consequences, Clin. Pharmacokinet. 9 (1984) 1–25.
[30] K.T. Le, H. Maurice, P. du Souich, First-pass metabolism of lidocaine in the anesthetized rabbit. Contribution of the small intestine, Drug Metab. Dispos. 24 (1996) 711–716.
[31] Y.K. Tam, Individual variation in first-pass metabolism, Clin. Pharmacokinet. 25 (1993) 300–328.
[32] T. Iwatsubo, N. Hirota, T. Ooie, H. Suzuki, N. Shimada, K. Chiba, T. Ishizaki, C.E. Green, C.A. Tyson, Y. Sugiyama, Prediction of in vivo drug metabolism in the human liver from in vitro metabolism data, Pharmacol. Ther. 73 (1997) 147–171.
[33] A.R. Boobis, D.S. Davies, Human cytochromes P-450, Xenobiotica 14 (1984) 151–185.
[34] A.R. Boobis, D.S. Davies, Multiple forms of human cytochrome P-450, Biochem. Soc. Trans. 12 (1984) 78–80.
[35] T. Lave, P. Coassolo, B. Reigner, Prediction of hepatic metabolic clearance based on interspecies allometric scaling techniques and in vitro–in vivo correlations, Clin. Pharmacokinet. 36 (1999) 211–231.
[36] T. Lave, B. Levet-Trafit, A.H. Schmitt-Hoffmann, B. Morgenroth, W. Richter, R.C. Chou, Interspecies scaling of interferon disposition and comparison of allometric scaling with concentration–time transformations, J. Pharm. Sci. 84 (1995) 1285–1290.
[37] J.B. Houston, D.J. Carlile, Prediction of hepatic clearance from microsomes, hepatocytes, and liver slices, Drug Metab. Rev. 29 (1997) 891–922.
[38] B.A. Saville, M.R. Gray, Y.K. Tam, Models of hepatic drug elimination, Drug Metab. Rev. 24 (1992) 49–88.
[39] B.A. Hoener, Predicting the hepatic clearance of xenobiotics in humans from in vitro data, Biopharm. Drug Dispos. 15 (1994) 295–304.
[40] T. Lave, S. Dupin, C. Schmitt, B. Valles, G. Ubeaud, R.C. Chou, D. Jaeck, P. Coassolo, The use of human hepatocytes to select compounds based on their expected hepatic extraction ratios in humans, Pharm. Res. 14 (1997) 152–155.
[41] T. Iwatsubo, H. Suzuki, N. Shimada, K. Chiba, T. Ishizaki, C.E. Green, C.A. Tyson, T. Yokoi, T. Kamataki, Y. Sugiyama, Prediction of in vivo hepatic metabolic clearance of YM796 from in vitro data by use of human liver microsomes and recombinant P-450 isozymes, J. Pharmacol. Exp. Ther. 282 (1997) 909–919.

[42] T. Iwatsubo, A. Hisaka, H. Suzuki, Y. Sugiyama, Prediction of in vivo nonlinear first-pass hepatic metabolism of YM796 from in vitro metabolic data, J. Pharmacol. Exp. Ther. 286 (1998) 122–127.

[43] J.J. Bogaards, E.M. Hissink, M. Briggs, R. Weaver, R. Jochemsen, P. Jackson, M. Bertrand, P.J. van Bladeren, Prediction of interindividual variation in drug plasma levels in vivo from individual enzyme kinetic data and physiologically based pharmacokinetic modeling, Eur. J. Pharm. Sci. 12 (2000) 117–124.

[44] G. Schneider, P. Coassolo, T. Lave, Combining in vitro and in vivo pharmacokinetic data for prediction of hepatic drug clearance in humans by artificial neural networks and multivariate statistical techniques, J. Med. Chem. 42 (1999) 5072–5076.

[45] K.S. Lown, J.C. Kolars, K.E. Thummel, J.L. Barnett, K.L. Kunze, S.A. Wrighton, P.B. Watkins, Interpatient heterogeneity in expression of CYP3A4 and CYP3A5 in small bowel. Lack of prediction by the erythromycin breath test, Drug Metab. Dispos. 22 (1994) 947–955.

[46] M.F. Paine, M. Khalighi, J.M. Fisher, D.D. Shen, K.L. Kunze, C.L. Marsh, J.D. Perkins, K.E. Thummel, Characterization of interintestinal and intraintestinal variations in human CYP3A-dependent metabolism, J. Pharmacol. Exp. Ther. 283 (1997) 1552–1562.

[47] J.C. Kolars, K.S. Lown, P. Schmiedlin-Ren, M. Ghosh, C. Fang, S.A. Wrighton, R.M. Merion, P.B. Watkins, CYP3A gene expression in human gut epithelium, Pharmacogenetics 4 (1994) 247–259.

[48] Y. Wen, R.P. Remmel, C.L. Zimmerman, First-pass disposition of (−)-6-aminocarbovir in rats. I. Prodrug activation may be limited by access to enzyme, Drug Metab. Dispos. 27 (1999) 113–121.

[49] D. Cong, M. Doherty, K.S. Pang, A new physiologically based, segregated-flow model to explain route-dependent intestinal metabolism, Drug Metab. Dispos. 28 (2000) 224–235.

[50] J. Baron, J.M. Voigt, Localization, distribution, and induction of xenobiotic-metabolizing enzymes and aryl hydrocarbon hydroxylase activity within lung, Pharmacol. Ther. 47 (1990) 419–445.

[51] W.H. Barr, S. Riegelman, Intestinal drug absorption and metabolism. I. Comparison of methods and models to study physiological factors of in vitro and in vivo intestinal absorption, J. Pharm. Sci. 59 (1970) 154–163.

[52] P.R. Gwilt, S. Comer, P.R. Chaturvedi, D.H. Waters, The influence of diffusional barriers on presystemic gut elimination, Drug Metab. Dispos. 16 (1988) 521–526.

[53] L.X. Yu, G.L. Amidon, Saturable small intestinal drug absorption in humans: modeling and interpretation of cefatrizine data, Eur. J. Pharm. Biopharm. 45 (1998) 199–203.

[54] P.B. Watkins, The barrier function of CYP3A4 and P-glycoprotein in the small bowel, Adv. Drug. Deliv. Rev. 27 (1997) 161–170.

[55] V.J. Wacher, C.Y. Wu, L.Z. Benet, Overlapping substrate specificities and tissue distribution of cytochrome P450 3A and P-glycoprotein: implications for drug delivery and activity in cancer chemotherapy, Mol. Carcinog. 13 (1995) 129–134.

[56] H. Suzuki, Y. Sugiyama, Role of metabolic enzymes and efflux transporters in the absorption of drugs from the small intestine, Eur. J. Pharm. Sci. 12 (2000) 3–12.

[57] A.T. Chow, W.J. Jusko, Application of moment analysis to nonlinear drug disposition described by the Michaelis–Menten equation, Pharm. Res. 4 (1987) 59–61.

[58] A.T. Chow, W.J. Jusko, Michaelis–Menten metabolite formation kinetics: equations relating area under the curve and metabolite recovery to the administered dose, J. Pharm. Sci. 79 (1990) 902–906.

[59] J. McAinsh, M.A. Gay, Theoretical Michaelis–Menten elimination model for propranolol, Eur. J. Drug Metab. Pharmacokinet. 10 (1985) 241–245.

[60] J. McAinsh, N.S. Baber, B.F. Holmes, J. Young, S.H. Ellis, Bioavailability of sustained release propranolol formulations, Biopharm. Drug Dispos. 2 (1981) 39–48.

[61] W. Sadee, V. Drubbisch, G.L. Amidon, Biology of membrane transport proteins, Pharm. Res. 12 (1995) 1823–1837.

[62] H. Han, R.L. de Vrueh, J.K. Rhie, K.M. Covitz, P.L. Smith, C.P. Lee, D.M. Oh, W. Sadee, G.L. Amidon, 5′-Amino acid esters of antiviral nucleosides, acyclovir, and AZT are absorbed by the intestinal PEPT1 peptide transporter, Pharm. Res. 15 (1998) 1154–1159.

[63] P.W. Swaan, B.C. Koops, E.E. Moret, J.J. Tukker, Mapping the binding site of the small intestinal peptide carrier (PepT1) using comparative molecular field analysis, Receptors Channels 6 (1998) 189–200.

[64] Y.M. Choi, S.M. Chung, W.L. Chiou, First-pass accumulation of salicylic acid in gut tissue after absorption in anesthetized rat, Pharm. Res. 12 (1995) 1323–1327.

[65] W.L. Chiou, We may not measure the correct intestinal wall permeability coefficient of drugs: alternative absorptive clearance concept, J. Pharmacokinet. Biopharm. 23 (1995) 323–331.

[66] K.S. Pang, M. Rowland, Hepatic clearance of drugs. II. Experimental evidence for acceptance of the 'well-stirred' model over the 'parallel tube' model using lidocaine in the perfused rat liver in situ preparation, J. Pharmacokinet. Biopharm 5 (1977) 655–680.

[67] R.W. Brauer, Liver circulation and function, Physiol Rev 43 (1963) 115–213.

[68] H.A. Semple, Y.K. Tam, R.T. Coutts, A computer simulation of the food effect: transient changes in hepatic blood flow and Michaelis–Menten parameters as mediators of hepatic first pass metabolism and bioavailability of propranolol, Biopharm. Drug Dispos. 11 (1990) 61–76.

[69] Q.Y. Zhang, D. Dunbar, A. Ostrowska, S. Zeisloft, J. Yang, L.S. Kaminsky, Characterization of human small intestinal cytochromes P-450, Drug Metab. Dispos. 27 (1999) 804–809.

[70] V.D. Makhey, A. Guo, D.A. Norris, P. Hu, J. Yan, P.J. Sinko, Characterization of the regional intestinal kinetics of drug efflux in rat and human intestine and in Caco-2 cells, Pharm. Res. 15 (1998) 1160–1167.

[71] T. Gramatte, R. Oertel, Intestinal secretion of intravenous

talinolol is inhibited by luminal R-verapamil, Clin. Pharmacol. Ther. 66 (1999) 239–245.
[72] S. Doppenschmitt, H. Spahn-Langguth, C.G. Regardh, P. Langguth, Role of P-glycoprotein-mediated secretion in absorptive drug permeability: An approach using passive membrane permeability and affinity to P-glycoprotein, J. Pharm. Sci. 88 (1999) 1067–1072.
[73] D.G. Shand, Pharmacokinetics of propranolol: a review, Postgrad. Med. J. 52 (1976) 22–25.
[74] B.M. Silber, N.H. Holford, S. Riegelman, Dose-dependent elimination of propranolol and its major metabolites in humans, J. Pharm. Sci. 72 (1983) 725–732.
[75] J.G. Wagner, Propranolol: pooled Michaelis–Menten parameters and the effect of input rate on bioavailability, Clin. Pharmacol. Ther. 37 (1985) 481–487.
[76] F. Keller, U. Kunzendorf, G. Walz, H. Haller, G. Offermann, Saturable first-pass kinetics of propranolol, J. Clin. Pharmacol. 29 (1989) 240–245.
[77] Y.A. Weiss, M.E. Safar, C. Chevillard, A. Frydman, A. Simon, P. Lemaire, J.M. Alexandre, Comparison of the pharmacokinetics of intravenous DL-propranolol in borderline and permanent hypertension, Eur. J. Clin. Pharmacol. 10 (1976) 387–393.
[78] E. Cid, F. Mella, L. Lucchini, M. Carcamo, J. Monasterio, Plasma concentrations and bioavailability of propranolol by oral, rectal, and intravenous administration in man, Biopharm. Drug Dispos. 7 (1986) 559–566.
[79] L.S. Olanoff, T. Walle, T.D. Cowart, U.K. Walle, M.J. Oexmann, E.C. Conradi, Food effects on propranolol systemic and oral clearance: support for a blood flow hypothesis, Clin. Pharmacol. Ther. 40 (1986) 408–414.
[80] U. Klotz, Clinical pharmacology of midazolam, Anaesthesiol. Reanim 14 (1989) 347–354.
[81] J.H. Kanto, Midazolam: the first water-soluble benzodiazepine. Pharmacology, pharmacokinetics and efficacy in insomnia and anesthesia, Pharmacotherapy 5 (1985) 138–155.
[82] H.H. Kupferschmidt, H.R. Ha, W.H. Ziegler, P.J. Meier, S. Krahenbuhl, Interaction between grapefruit juice and midazolam in humans, Clin. Pharmacol. Ther. 58 (1995) 20–28.
[83] S.M. Tsunoda, R.L. Velez, L.L. von Moltke, D.J. Greenblatt, Differentiation of intestinal and hepatic cytochrome P450 3A activity with use of midazolam as an in vivo probe: effect of ketoconazole, Clin. Pharmacol. Ther. 66 (1999) 461–471.
[84] L.L. von Moltke, D.J. Greenblatt, J. Schmider, S.X. Duan, C.E. Wright, J.S. Harmatz, R.I. Shader, Midazolam hydroxylation by human liver microsomes in vitro: inhibition by fluoxetine, norfluoxetine, and by azole antifungal agents, J. Clin. Pharmacol. 36 (1996) 783–791.
[85] J.S. Wang, X. Wen, J.T. Backman, P. Taavitsainen, P.J. Neuvonen, K.T. Kivisto, Midazolam alpha-hydroxylation by human liver microsomes in vitro: inhibition by calcium channel blockers, itraconazole and ketoconazole, Pharmacol. Toxicol. 85 (1999) 157–161.
[86] L.D. Bornemann, B.H. Min, T. Crews, M.M. Rees, H.P. Blumenthal, W.A. Colburn, I.H. Patel, Dose dependent pharmacokinetics of midazolam, Eur. J. Clin. Pharmacol. 29 (1985) 91–95.
[87] J.K. Aronson, Clinical pharmacokinetics of digoxin 1980, Clin. Pharmacokinet. 5 (1980) 137–149.
[88] D.J. Greenblatt, T.W. Smith, J. Koch-Weser, Bioavailability of drugs: the digoxin dilemma, Clin. Pharmacokinet. 1 (1976) 36–51.
[89] E. Iisalo, Clinical pharmacokinetics of digoxin, Clin. Pharmacokinet. 2 (1977) 1–16.
[90] B. Greiner, M. Eichelbaum, P. Fritz, H.P. Kreichgauer, O. von Richter, J. Zundler, H.K. Kroemer, The role of intestinal P-glycoprotein in the interaction of digoxin and rifampin, J. Clin. Invest. 104 (1999) 147–153.
[91] S.F. Su, J.D. Huang, Inhibition of the intestinal digoxin absorption and exsorption by quinidine, Drug Metab. Dispos. 24 (1996) 142–147.
[92] A.E. Kim, J.M. Dintaman, D.S. Waddell, J.A. Silverman, Saquinavir, an HIV protease inhibitor, is transported by P-glycoprotein, J. Pharmacol. Exp. Ther. 286 (1998) 1439–1445.
[93] R.M. Hoetelmans, P.L. Meenhorst, J.W. Mulder, D.M. Burger, C.H. Koks, J.H. Beijnen, Clinical pharmacology of HIV protease inhibitors: focus on saquinavir, indinavir, and ritonavir, Pharm. World Sci. 19 (1997) 159–175.
[94] V.A. Eagling, L. Profit, D.J. Back, Inhibition of the CYP3A4-mediated metabolism and P-glycoprotein-mediated transport of the HIV-1 protease inhibitor saquinavir by grapefruit juice components, Br. J. Clin. Pharmacol. 48 (1999) 543–552.
[95] H.H. Kupferschmidt, K.E. Fattinger, H.R. Ha, F. Follath, S. Krahenbuhl, Grapefruit juice enhances the bioavailability of the HIV protease inhibitor saquinavir in man, Br. J. Clin. Pharmacol. 45 (1998) 355–359.
[96] M.E. Fitzsimmons, J.M. Collins, Selective biotransformation of the human immunodeficiency virus protease inhibitor saquinavir by human small-intestinal cytochrome P4503A4: potential contribution to high first-pass metabolism, Drug Metab. Dispos. 25 (1997) 256–266.
[97] A. Hsu, G.R. Granneman, G. Cao, L. Carothers, T. el-Shourbagy, P. Baroldi, K. Erdman, F. Brown, E. Sun, J.M. Leonard, Pharmacokinetic interactions between two human immunodeficiency virus protease inhibitors, ritonavir and saquinavir, Clin. Pharmacol. Ther. 63 (1998) 453–464.
[98] K.L. Halifax, W.E. Lindup, G.M. Barry, H.R. Wiltshire, D.J. Back, Binding of the HIV protease inhibitor saquinavir to human plasma proteins, Br. J. Clin. Pharmacol. 46 (1998) 291.
[99] V. Bahr, R. Hansel, Immunomodulating properties of 5,20 alpha (*R*)-dihydroxy-6 alpha,7 alpha-epoxy-1-oxo-(5 alpha)-whitha-2,24-dienolide and solasodine, Planta. Med. 44 (1982) 32–33.
[100] J. Meier, Pharmacokinetic comparison of pindolol with other beta-adrenoceptor-blocking agents, Am. Heart J. 104 (1982) 364–373.
[101] W.A. Wargin, R.J. Sawchuk, J.W. McBride, H.G. McCoy, M.L. Rylander, Variable first-pass elimination of propranolol following single and multiple oral doses in hypertensive patients, Eur. J. Drug Metab. Pharmacokinet. 7 (1982) 183–189.
[102] G.C. Kane, J.J. Lipsky, Drug-grapefruit juice interactions, Mayo Clin. Proc. 75 (2000) 933–942.

[103] K.S. Lown, D.G. Bailey, R.J. Fontana, S.K. Janardan, C.H. Adair, L.A. Fortlage, M.B. Brown, W. Guo, P.B. Watkins, Grapefruit juice increases felodipine oral availability in humans by decreasing intestinal CYP3A protein expression, J. Clin. Invest. 99 (1997) 2545–2553.

[104] K.S. Lown, R.R. Mayo, A.B. Leichtman, H.L. Hsiao, D.K. Turgeon, P. Schmiedlin-Ren, M.B. Brown, W. Guo, S.J. Rossi, L.Z. Benet, P.B. Watkins, Role of intestinal P-glycoprotein (mdr1) in interpatient variation in the oral bioavailability of cyclosporine, Clin. Pharmacol. Ther. 62 (1997) 248–260.

[105] S. Madani, M.F. Paine, L. Lewis, K.E. Thummel, D.D. Shen, Comparison of CYP2D6 content and metoprolol oxidation between microsomes isolated from human livers and small intestines, Pharm. Res. 16 (1999) 1199–1205.

[106] L. Salphati, L.Z. Benet, Modulation of P-glycoprotein expression by cytochrome P450 3A inducers in male and female rat livers, Biochem. Pharmacol. 55 (1998) 387–395.